Can linear stability analyses predict the development of river bed waves with lengths much larger than the water depth?

Hermjan Barneveld[1,1], Erik Mosselman[2,2], Victor Chavarrias[3,3], and A.J.F. (Ton) Hoitink[4,4]

[1]Wageningen University and Research
[2]Deltares & Delft University of Technology
[3]Unknown
[4]Wageningen University

December 8, 2022

Abstract

Sustainable river management can be supported by models predicting long-term morphological developments. Even for one-dimensional morphological models, run times can be up to several days for simulations over multiple decades. Alternatively, analytical tools yield metrics that allow estimation of migration celerity and damping of bed waves, which have potential for being used as rapid assessment tools to explore future morphological developments. We evaluate the use of analytical relations based on linear stability analyses of the St. Venant-Exner equations, which apply to bed waves with spatial scales much larger than the water depth. With a one-dimensional numerical morphological model, we assess the validity range of the analytical approach. The comparison shows that the propagation of small bed perturbations is well-described by the analytical approach. For Froude numbers over 0.3, diffusion becomes important and bed perturbation celerities reduce in time. A spatial-mode linear stability analysis predicts an upper limit for the bed perturbation celerity. For longer and higher bed perturbations, the dimensions relative to the water depth and the backwater curve length determine whether the analytical approach yields realistic results. For higher bed wave amplitudes, non-linearity becomes important. For Froude numbers [?]0.3, the celerity of bed waves is increasingly underestimated by the analytical approach. The degree of underestimation is proportional to the ratio of bed wave amplitude to water depth and the Froude number. For Froude numbers exceeding 0.3, the net impact on the celerity depends on the balance between the decrease due to damping and the increase due to non-linear interaction.

Posted on 8 Dec 2022 — CC-BY-NC-ND 4 — https://doi.org/10.1002/essoar.10512969.2 — This a preprint and has not been peer reviewed. Data may be preliminary.

Can linear stability analyses predict the development of river bed waves with lengths much larger than the water depth?

H.J. Barneveld[1,4], E. Mosselman[2,3], V. Chavarrías[2], A.J.F. Hoitink[1]

[1]Wageningen University and Research, Hydrology and Quantitative Water Management Group, Department of Environmental Sciences, Droevendaalsesteeg 3, 6708 PB Wageningen, the Netherlands
[2]Deltares, P.O. Box 177, 2600 MH Delft, the Netherlands
[3]Delft University of Technology, Faculty of Civil Engineering and Geosciences, P.O. Box 5, 2600 AA Delft, the Netherlands
[4]HKV, Botter 11-29, 8232 JN Lelystad, the Netherlands

Key Points:

- Rapid assessment metrics from linear stability analysis predict the propagation of low bed waves provided that Fr $\leq$0.3.
- For Fr $>$0.3 bed waves are more diffusive and migrate slower in time than predicted from linear stability analysis.
- Linear stability analysis results can validate numerical models, which in turn may verify the validity range of the former.

Corresponding author: Hermjan Barneveld, `hermjan.barneveld@wur.nl`

Abstract

Sustainable river management can be supported by models predicting long-term morphological developments. Even for one-dimensional morphological models, run times can be up to several days for simulations over multiple decades. Alternatively, analytical tools yield metrics that allow estimation of migration celerity and damping of bed waves, which have potential for being used as rapid assessment tools to explore future morphological developments. We evaluate the use of analytical relations based on linear stability analyses of the St. Venant-Exner equations, which apply to bed waves with spatial scales much larger than the water depth. With a one-dimensional numerical morphological model, we assess the validity range of the analytical approach. The comparison shows that the propagation of small bed perturbations is well-described by the analytical approach. For Froude numbers over 0.3, diffusion becomes important and bed perturbation celerities reduce in time. A spatial-mode linear stability analysis predicts an upper limit for the bed perturbation celerity. For longer and higher bed perturbations, the dimensions relative to the water depth and the backwater curve length determine whether the analytical approach yields realistic results. For higher bed wave amplitudes, non-linearity becomes important. For Froude numbers ≤ 0.3, the celerity of bed waves is increasingly underestimated by the analytical approach. The degree of underestimation is proportional to the ratio of bed wave amplitude to water depth and the Froude number. For Froude numbers exceeding 0.3, the net impact on the celerity depends on the balance between the decrease due to damping and the increase due to non-linear interaction.

Plain Language Summary

The riverbed responds to climate change and human interventions such as engineering works and dredging. A pit resulting from dredging, for example, typically moves in a downstream direction through the river, like a wave in the bed elevation. These waves move much slower than water waves, which is why structures like groynes and embankments in the Rhine and Meuse Rivers still cause long-term riverbed erosion. For proper river management, understanding the development of the riverbed over shorter and longer timescales is paramount. Numerical models are often used to simulate these changes, but simulations for multiple decades can last several days. Therefore, more efficient alternatives are of interest. We developed a theoretical approach to assess the propagation and damping of bed waves from a simple equation. The results have been compared to numerical model runs. The results are valid for low bed waves and river reaches with gentle bed slopes. When bed slopes increase, the approach overestimates the propagation of low bed waves. For the Dutch Meuse River, the approach is promising for the mildly sloped Sand Meuse, but overestimates bed wave celerities on longer timescales for the steeper Border Meuse upstream.

1 Introduction

In lowland rivers, bed morphological processes at spatial scales much larger than the water depth are generally slower than hydrodynamic processes. The morphological changes on river reaches of tens of kilometers or more typically develop over a period of years to centuries, which is here referred to as the engineering timescale. The engineering timescale is relevant from a perspective of planning river interventions and operational river management, which is often focused on navigability, flood prevention and nature conservation. In the long term, the river bed develops towards a (quasi) equilibrium situation. De Vries (1975) introduced a morphological timescale for the development of longitudinal riverbed profiles. He and others (e.g. Dade & Friend, 1998; Church & Ferguson, 2015) showed that larger lowland rivers may take 10^3 to 10^5 years to adapt to permanent changes, for example at the downstream boundary. Here, we focus on the prediction of development of the riverbed in reaches of tens of kilometers of length or more

in the coming century, as a consequence of changes in sediment supply or river geometry and the hydrological regime. These changes can be the result of, for instance, sediment nourishments, dredging activities or river widening measures. We evaluate if and how analytical relations, resulting from linear stability analysis of the governing equations, can be used for morphodynamic prediction, based on a comparison with high-complexity numerical model results.

Several techniques are available for assessment of the long-term (quasi-) equilibrium river bed profiles. Arkesteijn et al. (2019) developed a method to predict the quasi-equilibrium channel bed profile in the backwater region of a river, as well as its dynamics. The method is efficient, as the transient phase does not have to be computed. At engineering timescales, the development of sediment transport and bed level change in time is particularly relevant, which cannot be readily inferred from a (quasi) equilibrium state. The run time of numerical morphological models simulating the initial response at engineering timescales is still long. Even for one-dimensional models, where parameters and variables are averaged over the cross-section, a single simulation for a river reach of a hundred kilometres and several decades may take hours, or even days. To address uncertainty of model input and to evaluate the consequences of climate change projections, multiple simulations are required, necessitating a stochastic or probabilistic approach (e.g. Van Vuren et al., 2005). Many techniques are being developed to speed up morphological simulations. Besides improvement of numerical solvers, efforts to improve model efficiency are focused on the development of a morphological acceleration factor (e.g. Lesser et al., 2004; Carraro et al., 2018), the reduction of spin-up time (e.g. Yossef et al., 2008), and simplification of governing equations such as the quasi-steady approach first introduced by De Vries (1965)). Arkesteijn et al. (2021) used the distinction of timescales from Arkesteijn et al. (2019) to set up a rapid numerical method that determines the mean transient channel response under stochastic controls.

Analytical solutions for reduced-complexity model equations offer potential to be used as rapid assessment methods. Linear stability analyses provide such solutions, based on the assumption of infinitesimal perturbations of the river bed and the flow. However, little is known about the extent to which these analytical solutions are valid when the assumption of infinitesimal perturbations fails. Linear stability analyses of river morphodynamics have been performed extensively during the last five decades. Colombini (2022) provides an overview of stability analyses related to bars, dunes and antidunes, ripples, and to transverse or oblique bed forms like sand ridges or diagonal dunes. James (2006) refers to bed waves for all these changes in bed elevation during aggradation-degradation cycles. The governing equations in linear stability analyses differ for bed wave scales smaller or larger than the water depth.

Kennedy (1963, 1969) and Nakagawa and Tsujimoto (1980) showed that small-scale periodic bedforms result from an instability phenomenon caused by a phase lag between bed geometry and local rates of sediment transport. As a consequence, for subcritical conditions, a linear stability analysis of the governing Saint-Venant equations in combination with an Exner equation (including an equilibrium sediment transport predictor) does not show an instability that would explain the development of ripples and dunes (Balmforth & Provenzale, 2001; Charru, 2011). Various researchers have studied how non-equilibrium sediment transport can explain the initiation of bedforms. Nakagawa and Tsujimoto (1984) used the Eulerian interpretation of a stochastic model for bed load transport (Nakagawa & Tsujimoto, 1980) in a linear stability analysis, to explain the early stage of bedform development. Bohorquez and Ancey (2015, 2016) and Bohorquez et al. (2019) incorporate a non-equilibrium sediment transport formulation in the Exner equation, to account for particle diffusion. Including diffusion captures the net effect of the irregular movement of particles inherent to the stochastic nature of bedload sediment transport, and development of bedforms at small spatial and temporal scales (Furbish et al., 2012a, 2012b; Roseberry et al., 2012; Lajeunesse et al., 2010, 2018; Ancey & Hey-

man, 2014; Martínez-Aranda et al., 2019). For this reason, existing linear stability analyses adopting the classical Exner equation do no yield tools for morphodynamic prediction of ripples and dunes.

Several studies focus on morphological prediction of bed waves with lengths much larger than the water depth. Grijsen and Vreugdenhil (1976) and Ponce and Simons (1977) performed linear stability analyses, starting from perturbations in the flow. De Vries (1965) derived characteristic migration celerities of flow and river bed disturbances, and Vreugdenhil (1982) performed a linear stability analysis of the equations for flow and sediment assuming quasi-steady circumstances, which simplifies the analysis. In the latter case, the time derivatives in the governing flow equations were neglected, which was justified by De Vries (1965) for small values of the Froude number. Sieben (1996), Lyn and Altinakar (2002) and Lanzoni et al. (2006) elaborated further on this line of linear stability analyses, concentrating on mountain rivers and thus transcritical (Froude numbers in the range 0.8-1.2) and supercritical flow conditions. Lanzoni et al. (2006) also addressed subcritical flow conditions. They performed numerical simulations to check the character of the analytical expressions for migration celerities of infinitesimal flow and bed waves, without performing a comprehensive quantitative comparison between analytical and numerical results. They found that the results of the linear stability analyses, in terms of the direction of wave propagation (upstream, downstream) and amplification or damping of perturbations, agree with numerical simulations for small perturbations. All these studies showed that, in contrast to the studies related to the initiation and growth of ripples and dunes, the classical Exner equation with well-known equilibrium sediment transport predictors such as Meyer-Peter and Müller (1948) and Engelund and Hansen (1967), proves adequate for linear stability analyses of bed waves with lengths larger than the water depth. None of these studies validated quantitatively the results of the analysis for non-infinitesimal bed perturbations.

The objective of this paper is to establish and understand the extent to which the results of linear stability analyses for bed waves longer than the water depth can be applied as rapid assessment tool for large-scale morphodynamic development in lowland rivers under varying discharges, where perturbations in the flow and the river bed are not infinitesimally small. We express the validity range in terms of the Froude number F and relative amplitude of the bed waves (ratio of amplitude to water depth). For the numerical simulations, the geometry and hydrology of the Meuse River in the Netherlands were adopted as a starting point, where subcritical flow conditions predominate. However, the initial and boundary conditions were varied to cover a wide range of subcritical flow conditions.

Our linear stability analysis differs slightly from previous studies in that the length of the perturbations is linked to the period of the flood wave. This variable length is introduced through a parameter E, which is further explained in Section 2. The analysis, based on linearisation of the terms in the governing equations, provides relations for migration celerity and damping of flow and bed waves. We test a solution that is consistent with the spatial-mode analysis of Grijsen and Vreugdenhil (1976), which differs from the temporal-mode analysis (e.g. Lanzoni et al., 2006). The analysis shows that the governing parameters agree with other analyses in terms of the Froude number, the degree of unsteadiness, the strength of bed friction, the wave length of the bed perturbation and the sediment load.

Hereafter, we compare the propagation and damping of bed waves from the stability analysis with results from a one-dimensional full-dynamic numerical model with which we simulated low-amplitude perturbations of the flow and the river bed. The initial and boundary conditions of the numerical simulations do not exactly match the linear stability analysis, because the latter represents an initial-value problem for an unbounded domain. Nonetheless, the numerical results provide a direct comparison to the analytical results. Additionally, simulations with larger (longer and higher) flow and bed

waves are used to define the range within which the analytical results may be used as a rapid assessment tool for morphological development in lowland rivers. Although the spatial-mode analysis forms the starting point of the paper, a comparison with the more frequently applied temporal-mode analysis is also performed.

The structure of the remainder of this paper is as follows. Section 2 describes the linear stability analysis, providing analytical expressions of migration celerity and damping. The same section introduces the numerical model ELV and describes the simulations performed. Results of the linear stability analysis, the comparison with numerical results and assessment of the validity range of the analytical relations are given in Section 3. Practical application of the results, comparison with the temporal-mode analysis and further simplification of the analysis are discussed in Section 4.

2 Methods

2.1 Model Equations

We consider unidirectional flow over an erodible bed and assume bed elevation and sediment transport per unit width to be averaged over local fluctuations. These local fluctuations may relate to bedforms that are incorporated into a roughness parameter. The one-dimensional governing equations describing flow and bed evolution read as:

$$\frac{\partial u}{\partial t} + u\frac{\partial u}{\partial x} + g\frac{\partial h}{\partial x} + g\frac{\partial z}{\partial x} = -g\frac{u^2}{C^2 h} \tag{1}$$

$$\frac{\partial h}{\partial t} + h\frac{\partial u}{\partial x} + u\frac{\partial h}{\partial x} = 0 \tag{2}$$

$$\frac{\partial z}{\partial t} + \frac{\partial s}{\partial x} = 0 \tag{3}$$

$$s = f(u) \tag{4}$$

which include the 1D Saint-Venant equations for conservation of mass and momentum of water (Eq. 1 and Eq. 2), the continuity equation for sediment (Eq. 3) and a capacity-limited sediment transport predictor (Eq. 4), implicitly assuming small bed slopes. The latter two equations together form the Exner equation. Herein:

t = time (s)
x = longitudinal co-ordinate (m)
u = water velocity averaged in a cross-section (m/s)
h = water depth (m)
z = bed level (m)
C = Chézy coefficient for hydraulic roughness ($m^{1/2}/s$)
s = sediment transport per unit of width (bulk volume) (m^2/s)
g = acceleration due to gravity (m/s^2)

This set of equations is used in dimensional form for engineering practice and form the basis for the linear stability analysis and the numerical models applied in this study.

2.2 Linear Stability Analysis

The theory of linear stability analysis provides insight in the physics of flow and sediment transport, and offers a first approximation of the celerity of migration and damping (or amplification) of bed perturbations. Table 1 presents an overview of existing theoretical one-dimensional analyses of river dynamics and morphodynamics for perturbations with wave lengths (much) larger than the water depth. The differences in existing analyses relate to details of the mathematical problem addressed in the study, and

the choice of the normal modes adopted for solving the linearized set of equations. Either the wave number k or the wave frequency ω is assumed complex, which will be further explained later in this section.

Table 1. Overview of existing theoretical 1D analyses of hydrodynamic and morphodynamic model equations in case of supra-bedform perturbations (wave length >> water depth). HY = hydrodynamic equations. MO = morphodynamic equations. ODE = ordinary differential equation. PDE = partial differential equations. u/s = upstream. d/s = downstream. Solutions proceed directly from boundary conditions, using a Laplace transform of the PDE, or based on substitution of exponential functions $exp(ik_r x - k_i x - i\omega_r t + \omega_i t)$ for an infinitely large domain.

Description	Equations	Substitution of exponential functions				Boundary conditions	References
		k_r	k_i	ω_r	ω_i		
Backwater effects	HY, ODE	-	-	-	-	$d/s+$ $\Delta(z+h)$	Bélanger (1828)
Flood propagation with temporal damping	HY, PDE	$2\pi/L$	0	$2\pi c/L$	$-4\pi^2 D/L^2$	-	Ponce and Simons (1977)
Flood propagation with spatial damping	HY, PDE	$2\pi/L$	$1/L_D$	$2\pi c/L$	0	-	Grijsen and Vreugdenhil (1976)
Propagation of infinitesimal perturbations	MO, PDE	$2\pi/L$	0	$2\pi c/L$	0	-	De Vries (1965), De Vries (1966)
Morphodynamic wave and diffusion character	MO, PDE	$2\pi/L$	0	$2\pi c/L$	$-4\pi^2 D/L^2$	-	Vreugdenhil (1982), Lanzoni et al. (2006)
Response to downstream water level	MO, PDE	-	-	-	-	$d/s+$ $\Delta(z+h)$	De Vries (1973), De Vries (1975)
Aggradation due to sediment overloading	MO, PDE	-	-	-	-	$u/s+$ Δs	Ribberink and Van der Sande (1985)
Present study	MO, PDE	$2\pi/L$	$1/L_D$	$2\pi c/L$	0	-	-

Our linear stability analysis starts by assuming small perturbation of water depth, flow velocity and bed level:

$$h = h_o + h'$$
$$u = u_o + u'$$
$$z = z_o + z'$$

The subscript $_o$ indicates the steady uniform reference situation. The superscript $'$ indicates a small perturbation to the steady uniform reference situation.

Substitution of these expressions for h, u and z in equations 1 to 4, and combining the equations to a single equation in one of the parameters, yields:

$$\frac{\partial^2 h'}{\partial t^2} + c\frac{\partial^2 h'}{\partial x \partial t} - D\frac{\partial^3 h'}{\partial x^2 \partial t} + M_1\frac{\partial^3 h'}{\partial t^3} + M_2\frac{\partial^3 h'}{\partial x \partial t^2} + M_3\frac{\partial^3 h'}{\partial x^3} = 0 \qquad (5)$$

where:

$c = 1.5u_o$ (m/s)

$D = \frac{h_o u_o}{2i_o}(1 - F^2 + \frac{1}{h_o}\left.\frac{\partial f(u)}{\partial u}\right|_o)$ (m^2/s)

$M_1 = \frac{u_o}{2gi_o}$ (s)

$M_2 = \frac{{u_o}^2}{gi_o}$ (m)

$M_3 = -\frac{{u_o}^2}{2i_o}\left.\frac{\partial f(u)}{\partial u}\right|_o$ (m^3/s^2)

$F = \left.\frac{u}{\sqrt{gh}}\right|_o$ (-)

Similar equations can be obtained for u' and z'. Eq. 5 can be solved analytically by assuming a periodic solution for the water depth of the form:

$$h' = h_o \hat{h} \times e^{i(kx+\omega t)} \tag{6}$$

where:

h_o = steady uniform water depth (m)
$\hat{h}$ = dimensionless depth amplitude function (-)
k = wave number (m^{-1})
ω= frequency (t^{-1})
$i = \sqrt{-1}$

Two approaches can be adopted to obtain a solution for the perturbed variables (Drazin & Reid, 2004), a temporal-mode analysis and a spatial-mode analysis. In the temporal-mode analysis, the frequency ω is assumed complex and the wave number is real and equal to $k_r = \frac{2\pi}{L}$, where L is the wave length. In the spatial-mode analysis, the wave number k is assumed complex and the wave frequency ω real and equal to $\omega_r = \frac{2\pi}{T}$, where T is the wave period. The complex roots, i.e. either ω or k, determine the propagation and damping of perturbations in the flow and at the riverbed.

Many of the studies in Table 1 adopted the temporal mode in the analysis, assuming the perturbation wave number real ($k_r = \frac{2\pi}{L}$). Drazin and Reid (2004) describe that the physical properties of spatial modes are closer to the instability phenomena observed in most experiments on parallel flow, compared to temporal modes. In this study we extend the spatial-mode analysis by Grijsen and Vreugdenhil (1976). The corresponding waves proceeding from a spatial-mode analysis can pragmatically be interpreted as governed by boundary conditions, which are important in engineering practice. Strictly speaking, however, this type of linear analysis does not build on boundary conditions, but rather on a solution in an unbounded domain. The choice of the period of the proxy for the upstream boundary condition, i.e. the flow time series, sets the wave length of bed perturbation in the river, which is further elaborated in Section 2.3.4. The solution (Eq. 6), with known wave period T and thus known ω_r represents this boundary condition.

Our approach allows a comparison between the results of the linear stability analysis and numerical simulations with a discharge time series at the upstream boundary and a bed perturbation as initial condition across the 1D model domain.

In the spatial-mode analysis, the wave number k is complex

$$k = k_r + ik_i \tag{7}$$

where k_r determines the migration celerity c of the water and bed waves,

$$c = -\frac{\omega}{k_r} \text{ (m/s)} \tag{8}$$

and k_i determines the damping of water and bed waves

$$L_d = \frac{1}{k_i} \text{ (m)} \tag{9}$$

L_d is called the relaxation or damping length over which the amplitude of a wave is damped by a factor e^{-1}. c and L_d are the characteristic wave properties. For convenience, the wave number is first made dimensionless.

$$\hat{k} = \hat{k}_r + i\hat{k}_i = kx_o \ (-) \tag{10}$$

in which the characteristic length scale x_o is defined as

$$x_o = \frac{Q_o T}{B_o h_o} = u_o T \text{ (m)} \tag{11}$$

Herein, Q_o is the undisturbed flow and B_o the undisturbed width. Substitution of Eq. (10) and the solution, Eq. (6), in Eq. (5) leads to a third-order algebraic equation in the dimensionless wave number $\hat{k}$:

$$\frac{\Psi}{2\pi F^3 E}(\hat{k})^3 + \frac{1}{F^3 E}(1 - F^2 + \Psi)(\hat{k})^2 - \frac{4\pi}{FE}\hat{k} + 3i\hat{k} - \frac{4\pi^2}{FE} + 4\pi i = 0 \tag{12}$$

with three governing dimensionless parameters; F, Ψ and E:

$$\Psi = n\frac{s_o}{q_o} = \quad \text{dimensionless transport parameter} \tag{13}$$

$$E = \sqrt{\frac{g^3 T^2}{C^4 h}}\ (-) \tag{14}$$

Herein, n is the power in the sediment transport relation $s = m\ u^n$. The parameter E describes the influence of unsteadiness and non-uniformity of the flow on a scale larger than the local flow depth. Grijsen and Vreugdenhil (1976) introduced this parameter in their analysis of the flow equations and they defined typical values of E. For tidal waves, E takes a value of about 10^2 and for flood waves, $E \approx 10^3 - 5\ 10^4$. In our analysis we deal with the flood wave scale, so values of E are large. In Section 2.3.4 and Section 3.3 it is explained that larger values for E mean larger values for the wave length of bed perturbations.

The solution of Eq. (12) consists of three roots for $\hat{k}$. These roots determine the characteristic wave properties (migration celerity and damping) of both water and bed waves. Two roots describe damping and propagation of water waves and the third root describes the damping and propagation of the bed wave. In subcritical conditions the migration celerity of bed waves is much lower than of water waves. Therefore the morphodynamic root can easily be identified. The real part of the roots describes the migration celerity of the waves (Eq. (15)) and the imaginary part describes the damping (Eq. (16)).

$$c = -\frac{2\pi u_o}{\hat{k}_r} \tag{15}$$

$$L_d = \frac{u_o T}{\hat{k}_i} = \frac{u_o E C^2 h^{1/2}}{\hat{k}_i g^{3/2}} \tag{16}$$

2.3 Numerical Model Simulations

2.3.1 Introduction

To assess the applicability of the results of the linear stability analysis, numerical model simulations are performed. As the linear stability analysis is based on infinitesimal perturbations, numerical simulations with such perturbations should agree with the theoretical results, at least for the initial values. Simulations with non-infinitesimal perturbations and on longer time scales may or may not agree with results from the linear stability analysis, which is here being verified. For this verification we concentrate on the propagation of bed waves. The results for the damping of bed waves are presented as well. However, the numerical diffusion of mathematical models may hamper a fair comparison with the damping from the linear stability analysis.

2.3.2 Model Description

The numerical modelling code ELV is selected (Chavarrías, Stecca, et al., 2019), which is a Matlab code for modelling morphodynamic processes on a one-dimensional

domain. ELV has been successfully applied in various studies and proved stable and accurate (Arkesteijn et al., 2019, 2021; Blom et al., 2017; Chavarrías, Arkesteijn, & Blom, 2019). ELV solves the full set of equations (1 through 4) in an uncoupled way, with an implicit Preissmann scheme for flow and a first-order forward Euler upwind scheme for morphology. This is called the unsteady model. The model can readily be used to test simplified models, in which terms in the Saint-Venant equations are neglected. This simplification is planned in a follow-up study, so ELV was chosen at this stage as the modelling framework.

A selection of the simulations with ELV was repeated using the extensively tested and widely applied SOBEK-RE model. This model with a less diffusive numerical scheme has been developed by Deltares in the Netherlands and was validated in numerous studies and applications (Ji et al., 2003). The main objective of validating ELV with SOBEK-RE is to verify whether numerical aspects, such as numerical diffusion, may hamper a comparison between results of a linear stability analysis and model simulations.

2.3.3 Model Set-Up

For performing simulations that can be compared to results from the linear stability analysis, a one-branch model was constructed with characteristics as in Table 2. The geometry is inspired by The Meuse River in the Netherlands. However, upper limits of bed slope and grain diameter exceed field values of the Meuse River, to cover also larger values of the Froude number F, while keeping the sediment transport constant.

Table 2. Model set-up for simulation with ELV

Characteristic	Value/description
model length	10-25 km
channel width (no floodplains) B	100 m
hydraulic roughness, Chézy value C	40 $\mathrm{m}^{1/2}\mathrm{s}^{-1}$
bed slope i_b	0.0001 to 0.0022
space step Δx	2.5-25 m
time step Δt	1-5 sec
sediment transport s	uniform sediment, transport predictor of Engelund and Hansen (1967)
grain diameter $D50$	0.002 to 0.35 m
upstream boundary conditions	time series for discharge and equilibrium sediment transport
downstream boundary condition	uniform flow conditions (stage-discharge relation for uniform flow)

The branch length was chosen long enough to prevent any impact of the model boundaries on the area of interest, i.e. the area where a bed perturbation propagates and dampens. It was chosen short enough to allow for reasonable simulation times, for a simulation period of 1 to 3 years. The smallest space step, for the simulations with infinitesimal bed perturbations, amounted to 2.5 m (see below). For these simulations with a duration of 1 year, a branch length of 10 km was selected. For simulations with larger bed perturbations, the space step could be enlarged. A branch length of 25 km was selected for 3-year period simulations. For exact comparison with the linear stability analysis results, a simple rectangular cross-section with fixed width was adopted. The width of 100 m was selected arbitrarily. A constant Chézy value of 40 $\mathrm{m}^{1/2}/\mathrm{s}$ was adopted, but could be changed if desired. Changing the Chézy value, while maintaining the same values for water depth, velocity, Froude number F and bed load Ψ, will change the bed slope, $D50$

and the parameter E. The linear stability analysis demonstrates that for small Froude numbers (<0.3) the impact of changes in bed slope, $D50$ and E on the relative celerity and damping of bed waves is negligible. This was confirmed by an additional simulation for F=0.2 and C=45 $m^{1/2}/s$ in the supplementary material (Barneveld, 2022).

The Froude number F is a key parameter in the linear stability analysis. In this study, we focus on rivers with Froude numbers for which decoupling of the equations for flow and sediment transport is possible in numerical simulations. De Vries (1973), Morris and Williams (1996), Sieben (1996), Sieben (1999) and Cui et al. (2005) show that this is possible if Froude numbers are smaller than 0.7 to 0.8. In this study, we selected the range of F between 0.1 and 0.6 for the numerical simulations. With the selected Chézy value of 40 $m^{1/2}/s$, the corresponding range in bed slope i_b is between 0.0001 and 0.0022. To select the space step, a sensitivity analysis was carried out for the model with a length of 25 km and a bed perturbation of 1 km in length. Simulations were carried out for Froude numbers of 0.4 and 0.6. The space step was reduced from 100 to 50, 25 and 12.5 m. The time step was reduced accordingly, maintaining the Courant–Friedrichs–Lewy or CFL condition below 1, to have sufficient numerical accuracy of the simulations. The analysis showed that the difference between a spatial step of 25 m and 12.5 m was negligible, so 25 m was small enough. A second criterion was to schematize the bed perturbation with at least 20 grid points. For the simulations performed, the minimum selected space step was therefore 2.5 m.

In the theoretical analysis, the sediment transport and its non-linear response to flow, expressed with the parameter n, are important. For a meaningful comparison between theory and numerical simulations, we selected a sediment transport predictor with an unequivocal value of n. Many sediment transport predictors are used in engineering practice. For this research the frequently used sediment transport predictor of Engelund-Hansen with n=5 was selected (Engelund & Hansen, 1967). This formula for total sediment transport does not account for a threshold of motion and is widely used for sand-bed rivers. To ease the comparison between results of the linear stability analysis and numerical modelling results, we use identical sediment transport formulas for all computations. We apply the Engelund-Hansen transport predictor for low and high Froude numbers and for fine as well as coarse bed material. The Engelund-Hansen predictor may not be the most appropriate formula for prediction of transport of coarse sediments, but is applied while using the value of $D50$ to reach the desired sediment transport capacity. We assume that the comparison between linear stability analysis and numerical modelling based on the non-linear predictor of Engelund-Hansen (n=5) will also be representative when other sediment transport predictors are used.

For subcritical flow, conditions are needed at the upstream boundary for flow and sediment transport. As the objective of the simulations is to simulate the migration of bed waves in the time-space domain, we schematize the bed wave as a perturbation of the bed. At the upstream boundary, an equilibrium sediment transport load is imposed, which means that the sediment load fed to the model equals the sediment transport capacity for the actual discharge at the first calculation point. This guarantees a stable riverbed in the upstream part of the model. To perturb the flow, a boundary condition is imposed composed of a base flow magnitude, a peak flow magnitude, and a wave period T. The linear stability analysis is based on a sinusoidal shape of perturbations, but in our numerical simulations we adopt a more natural shape of the hydrodynamic wave, based on the Dimensionless Unit Hydrograph (DUH) method. By doing so, the application in engineering practices can be better assessed, and we verified that the impact of this choice on the results is negligible. The relation for discharge Q, based on the gamma relation for the DUH method, reads (USDA, 2007):

$$Q = Q_{base} + (Q_p - Q_{base}) e^m \left[\frac{t}{t_p}\right]^m \left[e^{(-m(\frac{t}{t_p}))}\right] \tag{17}$$

with:

Q_p = peak discharge (m^3/s)
Q_{base} = base discharge (m^3/s)
e = Euler's number equal to 2.7183
m = gamma equation shape factor (-)
$\frac{t}{t_p}$= ratio of the time of DUH coordinate to time to peak of the DUH

With values of $m = 15$ and $t_p = 20$ days, we generate a discharge time series at the upstream boundary with repeating flood waves of an approximate duration of 25 days (T), interrupted by periods of approximately 20 days with base flow. Figure 1 shows an example for a flood wave with a base flow of 500 m^3/s and a peak discharge of 1,500 m^3/s, characteristic of the Meuse River in the Netherlands. Simulations with small perturbations of the base flow are performed as well (see Table 3 in Section 2.3.4).

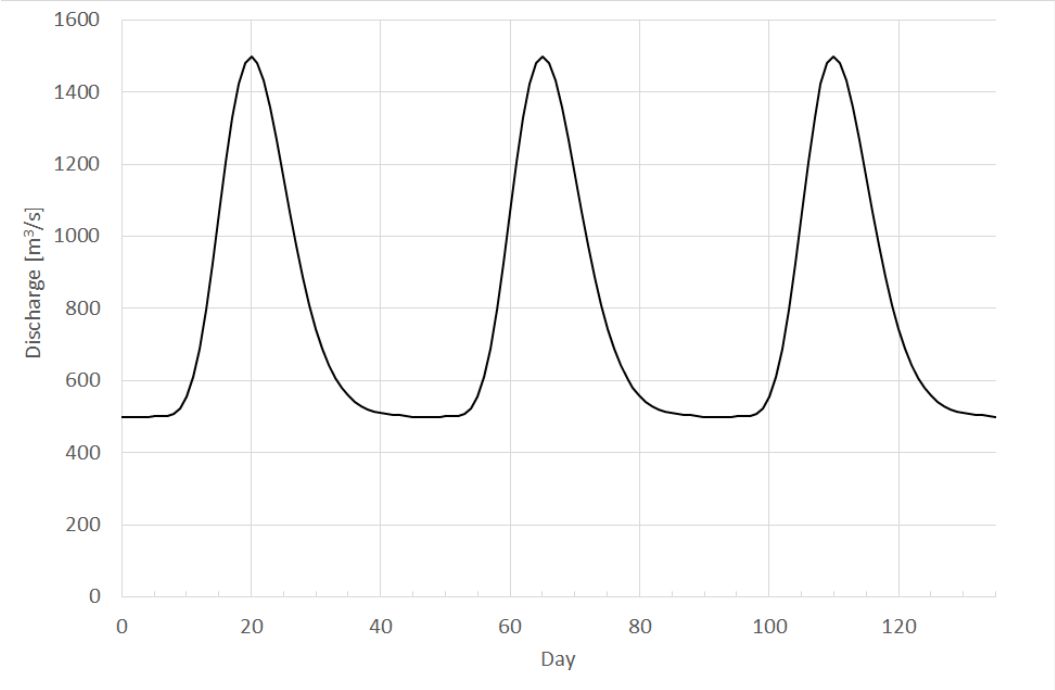


Figure 1. Sample flood wave boundary condition.

The wave period T of 25 days determines the parameter E in the governing equation of the linear stability analysis (Eqs. 12 and 14). Depending on the Froude number, E varies between 15,000 and 30,000 (for F=0.6). At the downstream boundary, one condition for the flow is required, for which the water level corresponding to normal flow is chosen.

2.3.4 Performed Simulations

Governing parameters in the linear stability analysis are F, E and Ψ. We are interested in the validity of the theoretically derived migration celerities for lowland rivers with Froude numbers up to 0.6 and hydrological conditions and sediment load characteristic for such environments. The parameter E is determined by the wave period of the flood wave, which we set at 25 days in a 45 days time domain. For the dimensionless transport parameter Ψ we adopted a value of $5.15 \cdot 10^{-5}$. Increasing the Froude number under conditions of constant Ψ means that the grain size increases.

First, we performed numerical simulations with small perturbations of the flow and the riverbed. We derived consistent combinations of the upstream boundary condition for flow and initial conditions for the bed perturbation. The wave period of the flow boundary condition determines the parameter E. With selected values of F and Ψ, the roots for the dimensionless wave number $\hat{k}$ (Eq. 10) can be determined, providing the migration celerity of the bed wave (Eq. 15). Eq. (8) and ω ($= \frac{2\pi}{T}$), which is known, determine the value of k_r, which sets the wave length L of the bed wave (using $k_r = \frac{2\pi}{L}$). In this way, wave lengths of the bed perturbation of 107 m (F=0.1) to 446 m (F=0.6) were derived.

To assess the validity of the results of the linear stability analysis for these infinitesimal perturbations at t=0, as well as for larger perturbations and for larger time scales (up to 3 years), a more elaborate set of simulations was performed, as summarized in Table 3.

Table 3. Numerical simulations performed to validate results from the linear stability analysis.

Set	Qbase[a] (m^3/s)	Qtop[b] (m^3/s)	Height[c] (m)	Length[d] (m)	Run duration (yr)	Comment
1	500	505	0.005	matching to flow (107-446 m)	1	base set
2	500	505	0.005	3000	3	long bed wave
3	500	1500	0.1-0.5	3000	3	large flow and bed waves

[a]base flow boundary condition
[b]peak flow boundary condition
[c]height bed perturbation (bed wave)
[d]wave length bed perturbation (bed wave)

3 Results

3.1 Migration Celerity Inferred From Linear Stability Analysis

The migration celerity of flow and bed waves follows from Eq. 15. For the bed waves, the dimensionless relative celerity is analyzed, which reads:

$$c_{rel} = \frac{c}{u_o} = -\frac{2\pi}{\hat{k}_r} \tag{18}$$

Figure 2 shows the results of this relative celerity for various combinations of E, F and Ψ. Figure 2 shows that for values of Ψ equal to or below $1{\cdot}10^{-5}$, the results are insensitive to E when Froude numbers are below 0.6. The results for different values of E are very similar for these conditions. When sediment transport increases, the parameter E becomes more important. When E increases, the relative celerity decreases and may (especially for larger values of Ψ) even decrease with increasing Froude numbers. This is due to the increasing diffusive character of bed waves, causing a decrease in the migration celerity of bed perturbations when Froude numbers increase. This has previously been described by Lisle et al. (2001) and Lanzoni et al. (2006), and will be elaborated on in Section 3.2.

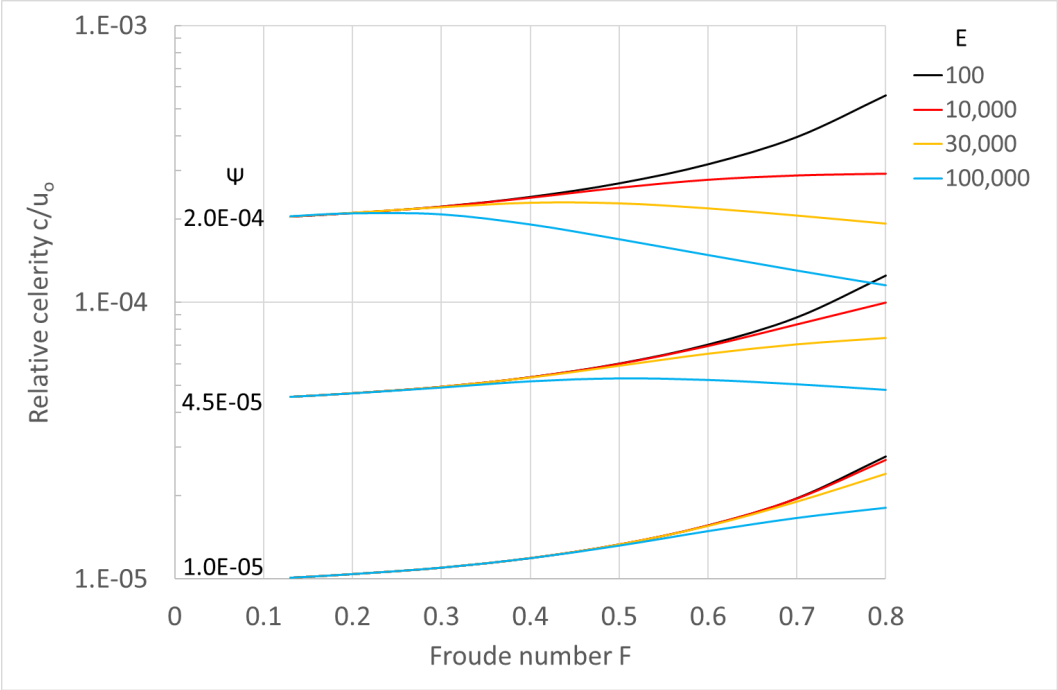


Figure 2. Relative celerity of bed waves in the linear stability analysis.

Figure 3 illustrates a Ψ value typical for lowland rivers, such as the River Meuse in the Netherlands. This case is used for the comparison with the numerical results in the next section.

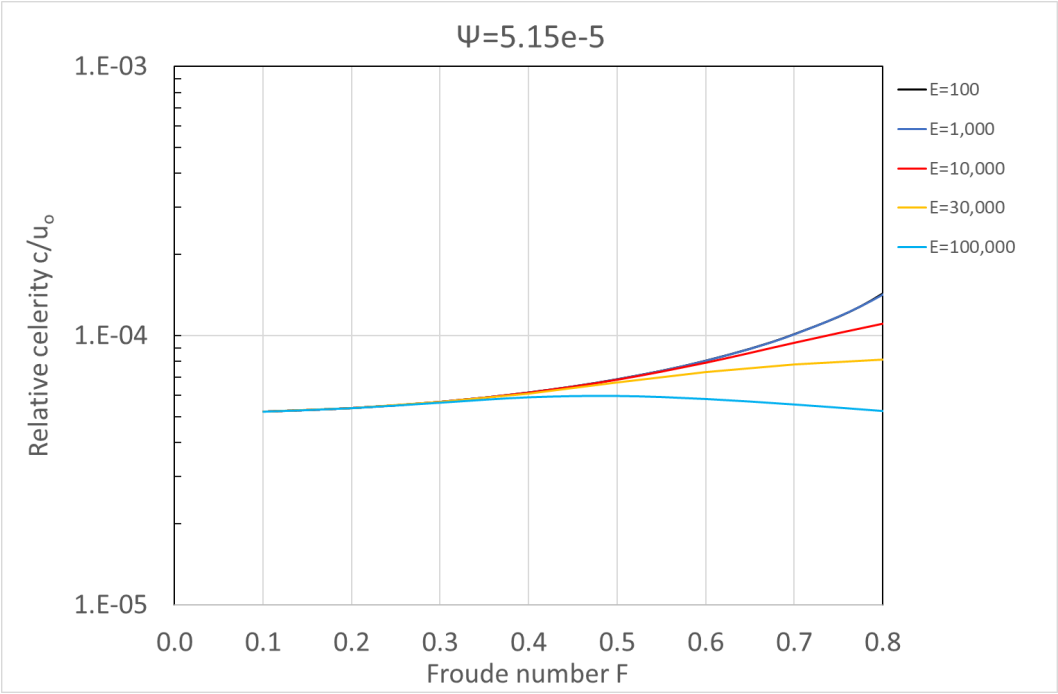


Figure 3. Relative celerity of bed waves in the linear stability analysis for $\Psi = 5.15 \cdot 10^{-5}$.

3.2 Numerical Modelling Results

From the simulations with a hydraulic upstream boundary condition and initial perturbation of the riverbed, the propagation of this bed perturbation was simulated for 3 consecutive periods of 45 days. In each period, a flood wave of 25 days occurred (Figure 1). The period of 45 days was selected by taking the Meuse River in the Netherlands as an example, where the annual sediment transport is known to be mainly concentrated in a period of this duration, normally in the winter season.

Figures 4 and 5 give examples of the propagation of the initial perturbation of the riverbed for Froude numbers of 0.2 and 0.6, respectively. The figures show that for F=0.2 the bed perturbation clearly translates in downstream direction, while damping takes place. For F=0.6 translation is small and diffusion of the bed perturbation in time dominates.

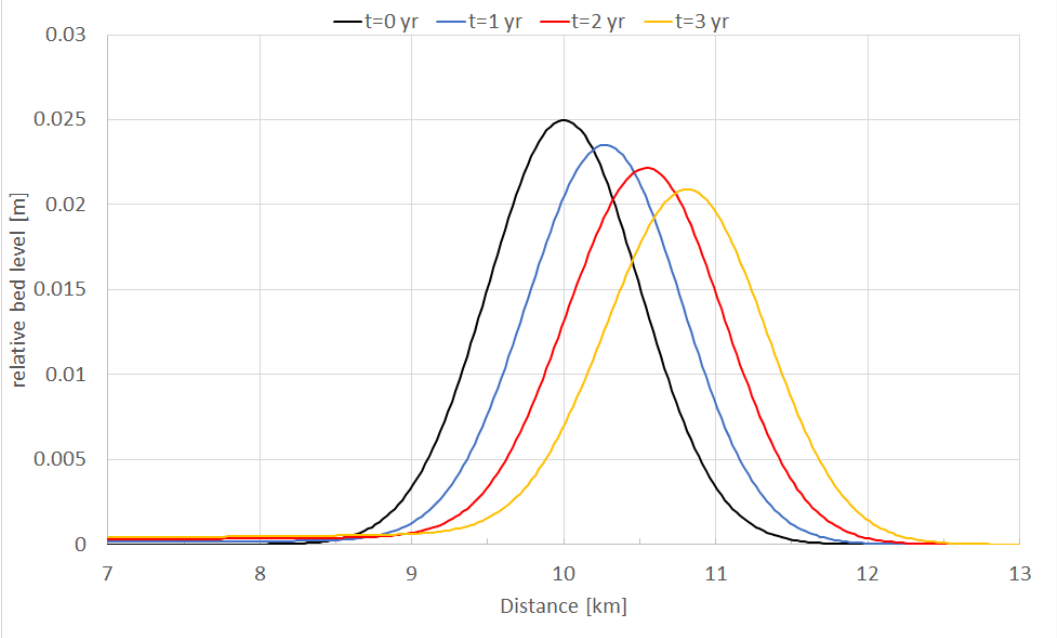


Figure 4. Simulated relative bed level (relative to bed slope) of a bed wave for F=0.2. The space step in this simulation was 25 m.

The differences in translation for different Froude numbers have been studied further by analyzing the migration celerity of the bed perturbations during the initial stage of the simulations. Again, a simulation period of 45 days was chosen for this analysis. Results for F between 0.2 and 0.6 are presented in Figures 6 and 7, respectively, showing the migration celerity of the crest of a bed perturbation in time. Figure 6 shows that for F=0.2 the bed perturbation migrates at a constant speed. For F=0.6 (Figure 7) the speed of the bed perturbation is more than halved in the 45 days of simulation.

The results of the ELV simulations for higher Froude numbers, F=0.4 and 0.6, were tested with the one-dimensional numerical model SOBEK-RE. The simulations with SOBEK-RE, with identical boundary conditions, setting of numerical parameters and time and space step, showed a similar diffusive character of bed perturbations for high Froude numbers. This supports the results of the ELV simulations.

Lisle et al. (2001) studied translation and diffusion for gravel-bed rivers. They based their analysis on the MPM (Meyer-Peter & Müller, 1948) bed load transport predictor,

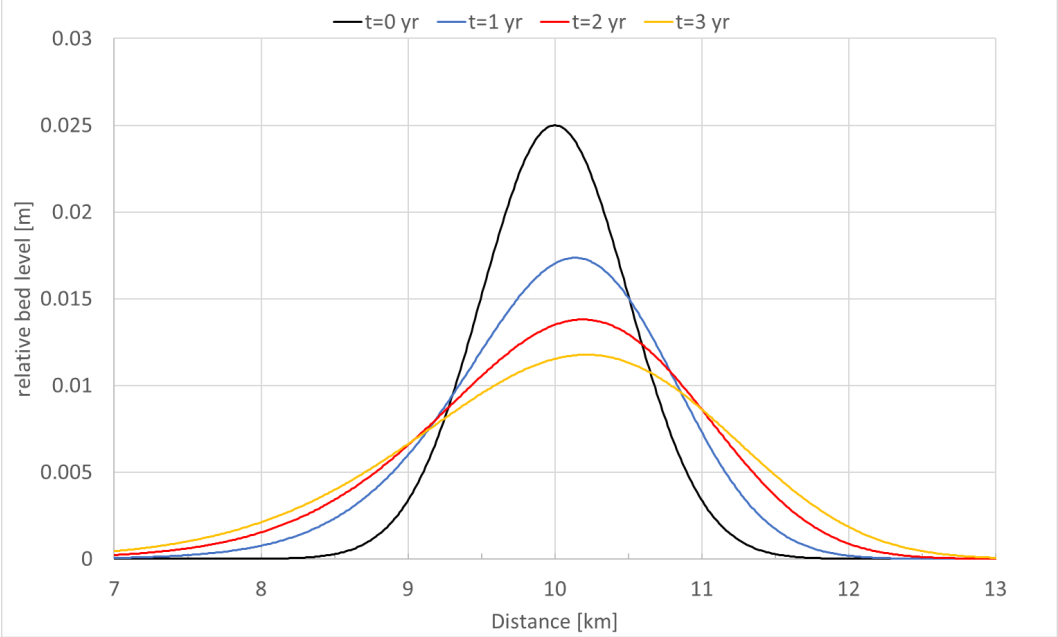


Figure 5. Simulated relative bed level (relative to bed slope) of a bed wave for F=0.6. The space step in this simulation was 25 m.

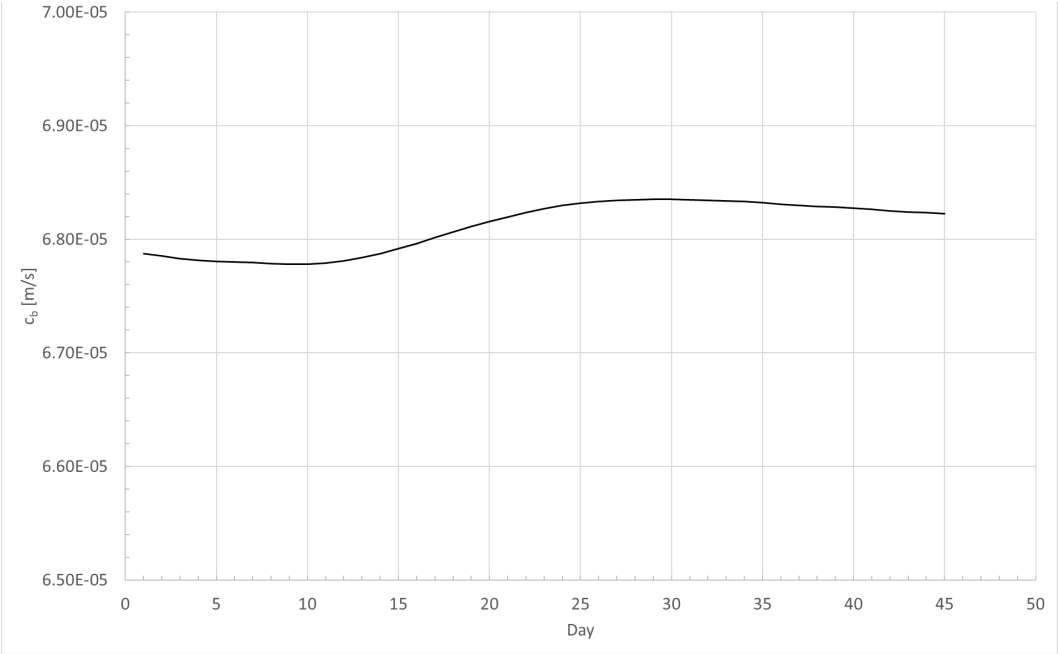


Figure 6. Simulated migration celerity c_b of the peak of the bed wave in first year for F=0.2.

but results provide general aspects of wave behaviour for other transport predictors as well. They present the following equation separating terms associated with translation of bed perturbations from those associated with diffusion.

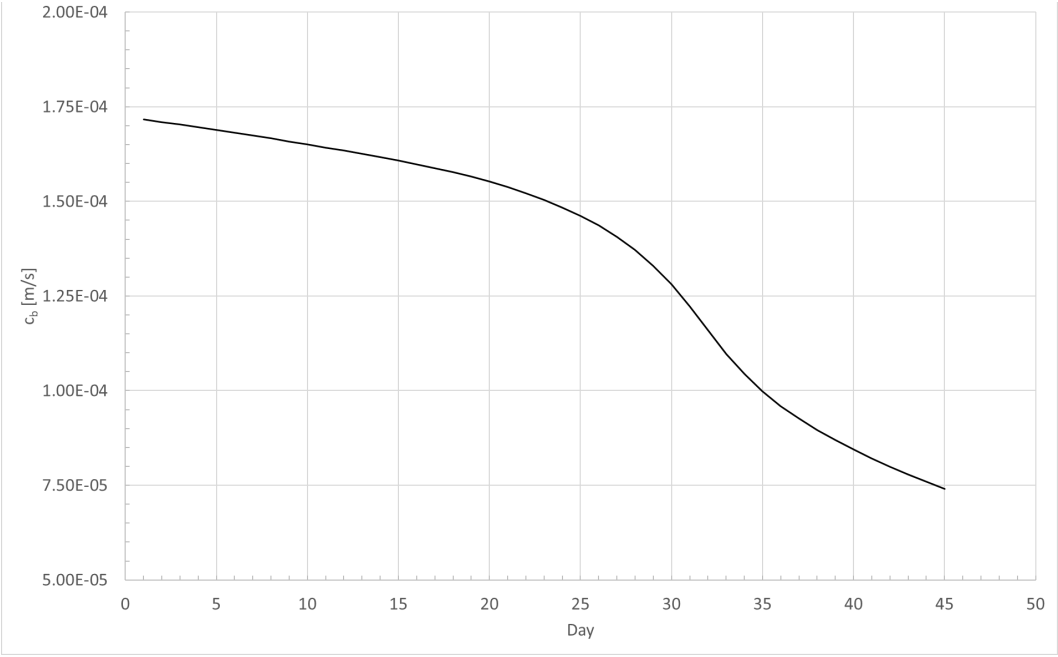


Figure 7. Simulated migration celerity c_b of the peak of the bed wave in first year for F=0.6.

$$\frac{\partial z}{\partial t} = \frac{K q c_f^{1/2}}{R_s(1-p)} \left[\frac{\partial z^2}{\partial x^2} + \left(\frac{\partial}{\partial x}(1-F^2)\frac{\partial h}{\partial x} \right) + ... \right] \tag{19}$$

where K is an empirical constant in the MPM equation, q is the unit water discharge, p is the bed porosity and R_s is the submerged specific gravity of sediment. The unspecified terms within the brackets are non-uniform flow terms, which are small for F<1. The first term within the brackets expresses the rate of wave diffusion. The second term expresses the rate of translation. The term 1-F^2 clearly indicates that translation decreases with increasing F. For those cases, diffusion dominates. Physically, this means that diffusion becomes more important when the dimensions of bed perturbations (i.e. height and wave length) become significant compared to the flow characteristics (i.e., the water depth and the length of backwater curve). This explains that for large Froude numbers, with smaller water depth and shorter backwater curves (i.e. Figure 5), diffusion of a bed wave is larger than for conditions with small Froude numbers (i.e. Figure 4). It is also in agreement with the reduced relative celerities in Figure 2 for larger values of E and F. Section 3.3 considers how diffusion changes the results from the linear stability analysis.

Lisle et al. (2001) also refer to a well-documented example for the Navarro River in California in 1995 (Sutherland et al., 2002). Landslide material that entered the steep gravel-bed river (bed slope of 0.0028), formed a bed wave that dispersed upstream and downstream and mostly disappeared within a few years with no measurable translation.

3.3 Comparison between Linear Stability Analysis results and Numerical Simulations

The results from the numerical simulations are compared with the results from the linear stability analysis in Figure 8. The figure shows that for both values of Ψ results of the linear stability analysis and numerical simulations agree for infinitesimal pertur-

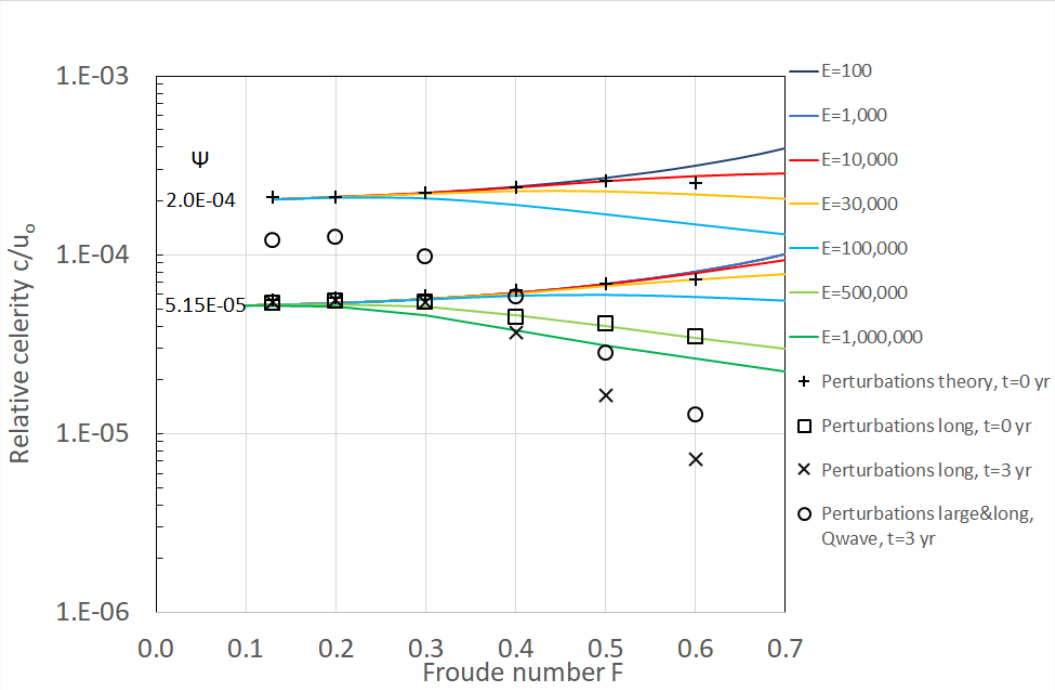


Figure 8. Comparison between relative celerities of bed perturbations from linear stability analysis (lines) and numerical simulations (markers) for $\Psi = 2 \cdot 10^{-4}$ and $\Psi = 5.15 \cdot 10^{-5}$.

bations with a wave length coupled to the value of E, at t=0 (+ markers; Perturbations theory, t=0 yr). The numerical results are in good agreement with the area delimited by the lines for E=10,000 (F=0.1) and E=30,000 (F=0.6). When the wave length of bed perturbations increases to 3,000 m (open box markers; Perturbations long, t=0 yr) the simulated initial migration celerities decrease for Froude numbers of 0.4 and higher. This is due to the increased diffusive character of the bed wave, as explained in the previous section. The linear stability analysis captures this. As already mentioned in Sections 2.2 and 2.3.4, the period of the upstream boundary condition and the wave length of bed perturbation in the river are coupled in the linear stability analysis. This means that the parameter E and wave length L are coupled, which is manifest as a relation in Figure 9. For moderate Froude numbers, up to 0.3, this relation is close to linear. For higher Froude numbers, the increase in parameter E accelerates with increasing wave length L.

For $\Psi = 5.15 \cdot 10^{-5}$ the validity range of the results of the linear stability analysis was assessed further. By choosing a wave length of 3,000 m, the parameter E increases to 350,000-500,000 for the range of Froude numbers considered. Figure 8 shows that for Froude numbers under 0.3 the impact of longer bed perturbations on the migration celerity is small, as the dependence on E is small. The simulated migration celerities of bed perturbations are fairly constant in time (Figure 6) and agree with results from the linear stability analysis. For Froude numbers up to and including 0.6, the linear stability analysis still predicts the initial migration celerities quite accurately when adopting E=500,000. For Froude numbers of 0.4 and higher the diffusive character is such that the wave length in time increases (Figure 5), the value of E increases (Figure 9) and the migration celerity thus decreases. The migration celerity from the linear stability analysis is an upper limit, and the deviation from the real migration celerity increases in time (x markers; Perturbations long, t=3 yr). This decrease in time is clearly shown in Figure 7.

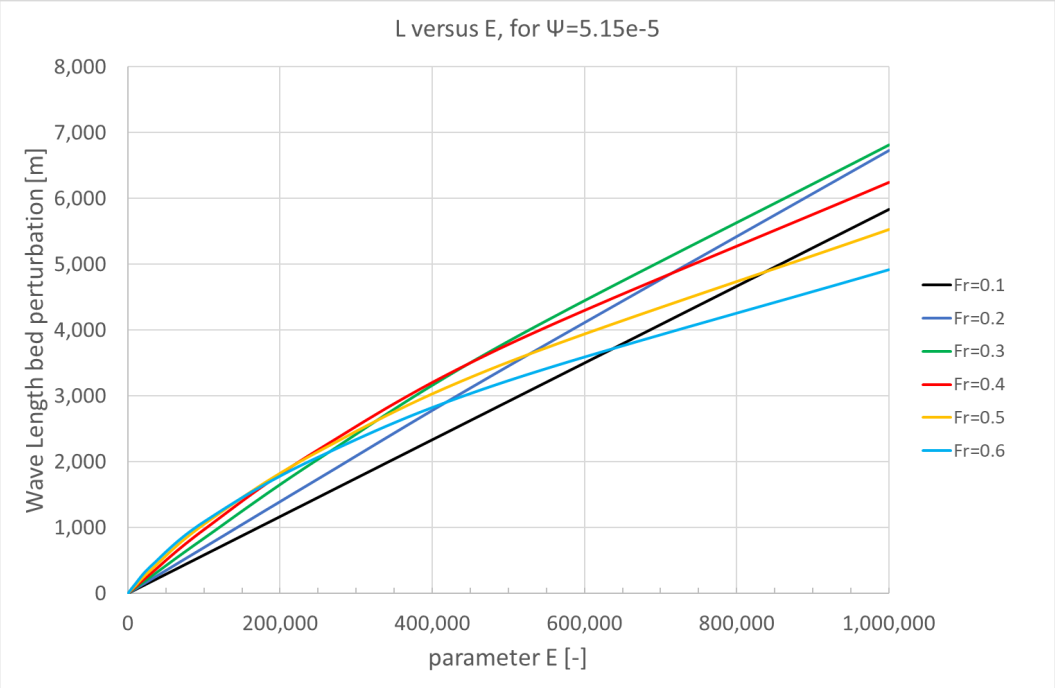


Figure 9. Relation between wave length L and parameter E in the linear stability analysis for $\Psi = 5.15 \cdot 10^{-5}$.

When the flow variations and perturbations in the bed are large (in height and length), the deviations between linear stability analysis and numerical results increase. The open circle markers (Perturbations large&long, t=3 yr) in Figure 8 represent simulations with a peak of the flood wave of 1,500 m^3/s (base flow = 500 m^3/s) and bed waves of 50 cm for F=0.1-0.4 and 10 cm for F=0.5-0.6. Under those conditions, the relative celerities increase compared to the simulations with small perturbations in the bed profile and the flow. This can be explained by the value of Ψ, which increases when the discharge in the simulations increases. In Figure 10, the simulation results with large perturbations of Figure 8 have been repeated, and results from the linear stability have been added when values of Ψ are based on the average sediment transports during the simulation (filled circle markers). The increase of values for Ψ brings results from the linear stability analysis and numerical simulations closer, especially for moderate Froude numbers (F=0.1-0.3). However, the relative celerities in this range of Froude numbers are still underestimated by the linear stability analysis. The increased non-linear effects due to the larger perturbations of the flow and the riverbed are responsible for this and, as expected, not reproduced by the linear stability analysis. This is further elaborated upon in the next section and in Figure 14.

3.4 Damping of Bed Waves

From the linear stability analysis (Eq. 16) and the numerical simulations, the damping length or relaxation length of bed waves can be derived. From the conditions and simulation related to $\Psi = 5.15 \cdot 10^{-5}$ (Figure 8) the results for the damping are presented in Figure 11. For the infinitesimal and relatively short bed waves (+ marker, Perturbations theory), the simulations show much more damping for Froude numbers up to 0.4. For longer and higher bed waves, the results from the linear stability analysis and numerical simulations show better agreement (values of E are in the range of 350,000 to 500,000).

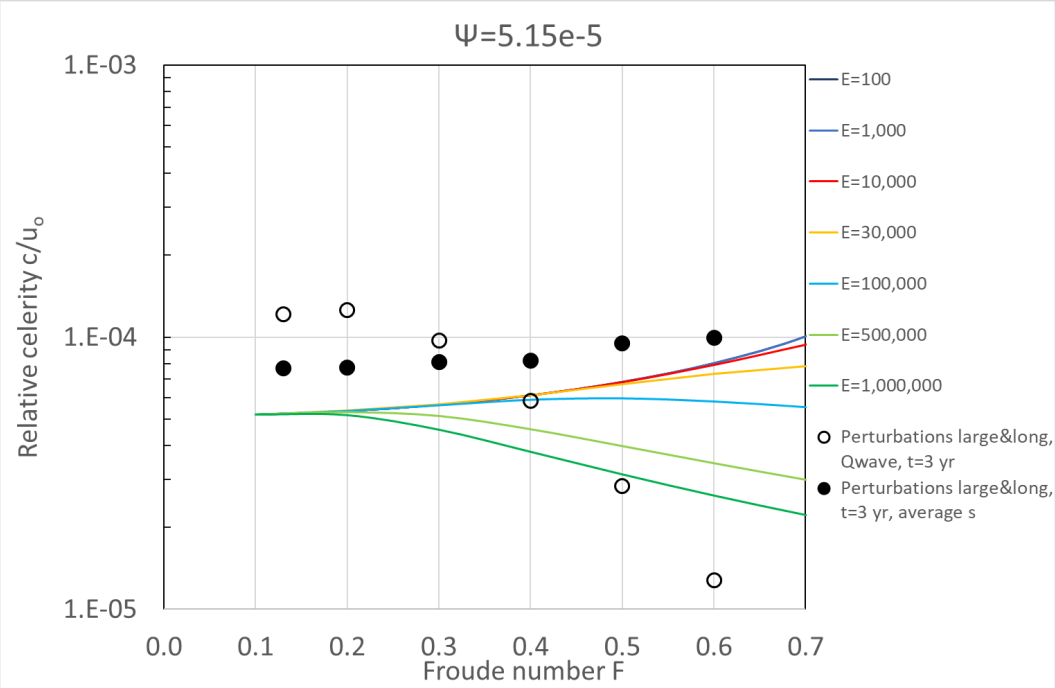


Figure 10. Relative celerity of large bed perturbations: linear stability analysis results based on initial sediment transport (solid lines) and based on average sediment transport during the simulations (filled circles), compared to the numerical results (open circles). Values of Ψ increase up to $7.0 - 7.5 \cdot 10^{-5}$.

4 Discussion

Strictly speaking, the mathematical problems solved by the linear stability analysis and numerical computation are not equivalent. The linear stability analysis solves an initial-value problem, whereas the numerical computation requires an initial condition and boundary conditions. Moreover, the flood waves used as boundary conditions in the numerical computations deviate from the harmonic functions assumed in the linear stability analysis. We have assumed that this does not seriously alter key characteristics such as migration celerity and damping.

The predictive value of the analytical approach is large when the diffusive character of bed waves is small, which appears to be related to the Froude number. For Froude numbers up to 0.3, diffusion of bed perturbations is normally small and migration celerities derived from the linear stability analysis are representative, even on longer time scales. This agrees with a threshold of F equal to 0.4 for translation in uniform sediment found by Lisle (2007). When dimensions of the bed perturbations increase compared to the depth and the backwater length, the diffusive character of bed waves increases. Nonetheless, linear stability analysis can still provide a good estimate of the initial migration celerity of bed perturbations. However, as the wave length of a bed perturbation grows in time, the appropriate parameter to be selected in the linear stability analysis also changes. The initial choice of the parameters overestimates the migration celerity of bed perturbations in time when the Froude number exceeds 0.3. The importance of the Froude number and relative dimensions of the bed perturbations confirms results from Lisle et al. (2001) and the theoretical analysis by Vreugdenhil (1982). The diffusion coefficient D, defined by Vreugdenhil (1982) as $D{=}\frac{1}{3}C^2\Psi h^2/u$, the wave number k and the migration celerity c determine how diffusive the system is. Therefore, the Péclet number $P{=}cL/D$

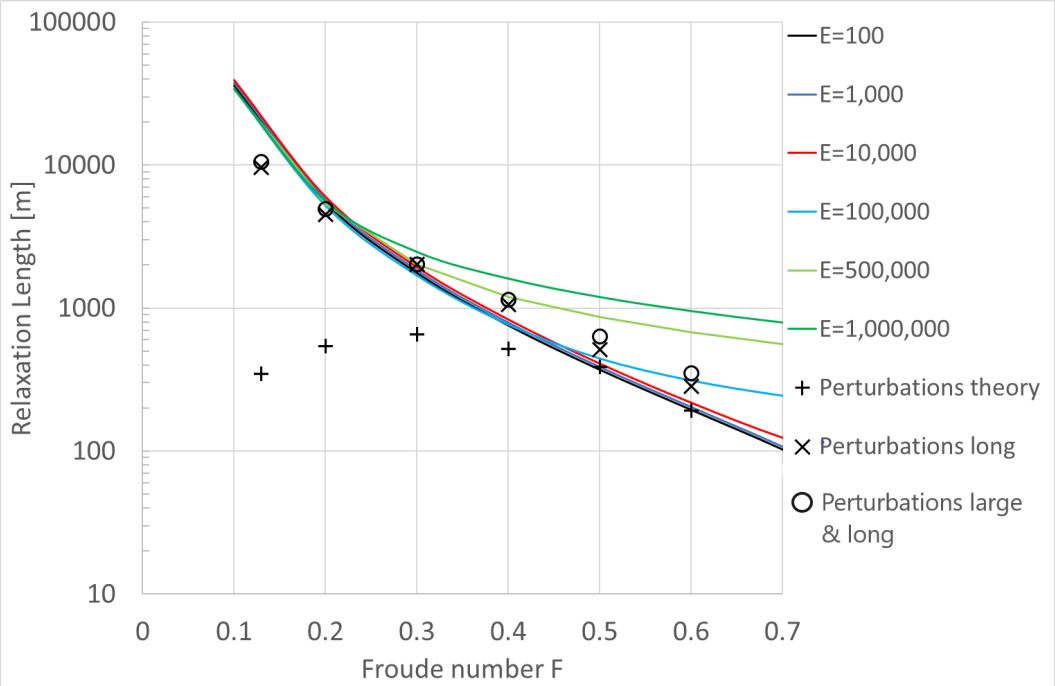


Figure 11. Comparison between damping of bed perturbations from linear stability analysis (lines) and numerical simulations (markers) for $\Psi = 5.15 \cdot 10^{-5}$. 'Perturbations theory' represent infinitesimal perturbations with a wave length coupled to the value of E. For the other simulations the wave length increased to 3,000 m, while for 'Perturbations large & long, Qwave' the bed wave amplitude increased and a flood wave was applied.

(where L is the wave-length) is relevant, which can be considered as the ratio of advection to the rate of diffusion. For high values of P, the system behaves as a pure diffusion equation and, vice versa, as a pure convection equation when P is small. Of course, the wave length of a convective wave can grow in time and diffusion will increase. Importantly, the Froude number F and Péclet number P are related. For high Froude numbers, backwater curves are short. The wave length of bed waves thus becomes relatively long, compared to the backwater curve.

G. Seminara (pers. comm., 2021) proposed that a more simple analytical expression for the relative celerity of bed waves may be possible, given that two of the determining parameters in the analysis are either very small (Ψ) or very large (E). As this insight was not published previously, we elaborated this further. When we expand the solution for the dimensionless wave number as

$$\hat{k} = \frac{\hat{k}_{-1}}{\Psi} + \hat{k}_0 + \hat{k}_1 \Psi + \dots , \tag{20}$$

we express E in terms of Ψ assuming that

$$E = \frac{E_0}{\Psi} \tag{21}$$

and we stop at the leading order, Eq. 12 can be written as:

$$(\hat{k}_{-1})^2 + 2\pi(1 - F^2)\hat{k}_{-1} + 6i\pi F^3 E_o = 0 \tag{22}$$

The solution reads:

$$\hat{k}_{-1} = \pi(1-F^2)\left[-1 \pm \sqrt{1 - i\frac{6}{\pi}\frac{E_o F^3}{(1-F^2)^2}}\right] \tag{23}$$

With Eq. 18, the relative celerity for the bed wave can be assessed again. Combining this with Figure 2 yields Figure 12. The results are almost identical, meaning that Eq. 23 indeed can be used for lowland rivers.

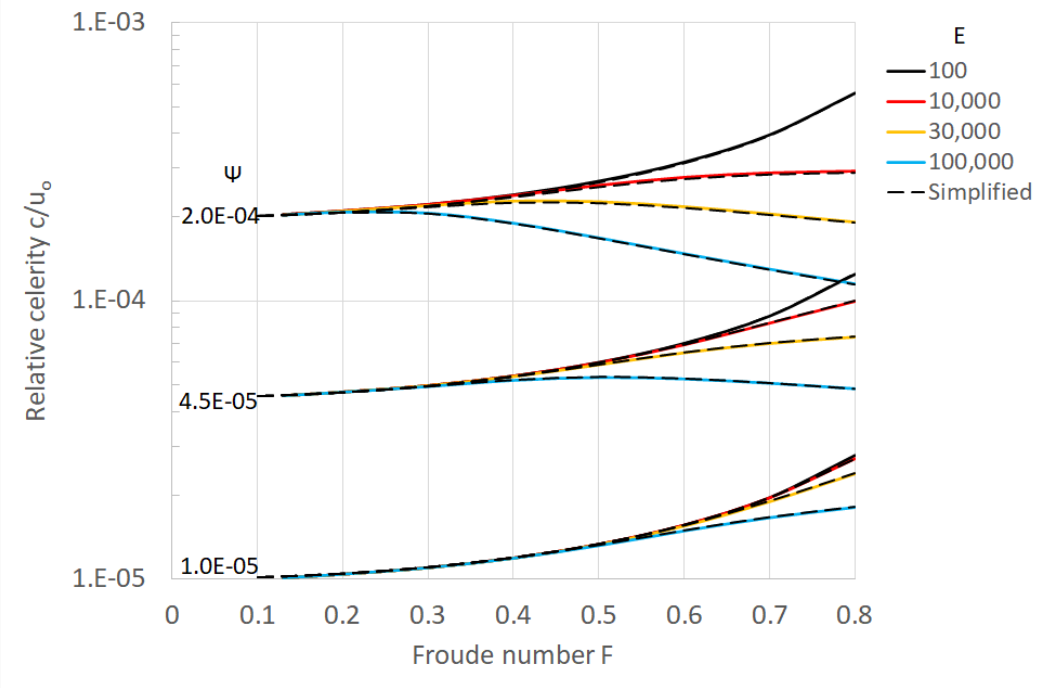


Figure 12. Relative celerity of bed waves: comparison of simplified results (black dotted line, Eq. 23) with original results of Figure 2.

In our analysis so far, we performed a spatial-mode analysis because it fits more closely to boundary-value problems solved by numerical models. A temporal-mode analysis is briefly elaborated upon for comparison. In the temporal-mode analysis, Eq. (12) transforms into an equation for the dimensionless complex frequency $\hat{\omega}$.

$$F^2(\hat{\omega})^3 + (2i - 2\hat{L}F^2)(\hat{\omega})^2 + (-3\hat{L}i - (\hat{L})^2(1 - F^2 + \Psi))\hat{\omega} + (\hat{L})^3\Psi = 0 \tag{24}$$

where:

L = wave length of disturbance (m)
$L_o = \frac{h_o}{i_o}$ (m)
$\hat{L} = 2\pi\frac{L_o}{L}$ (-)
$\hat{\omega} = \hat{\omega}_r + i\hat{\omega}_i$ = dimensionless complex frequency

Herein, $\hat{\omega}_i$ determines the damping of water and bed waves:

$$L_d = -\frac{c}{\hat{\omega}_i} \tag{25}$$

and $\hat{\omega}_r$ determines the migration celerity of the water and bed waves, according to:

$$\hat{c} = \frac{c}{u_o} = \frac{\frac{L}{T}}{u_o} = \frac{\hat{\omega}_r}{\hat{k}}. \tag{26}$$

Solving Eq. 24 again provides the roots determining propagation and damping of disturbances of flow and at the bed. The character of this equation agrees with the derivation of Lanzoni et al. (2006) (their Eq. 14).

Figure 13 presents the results of the linear stability analyses adopting spatial and temporal modes, as well as the simulated results. Both spatial-mode and temporal-mode analyses accurately predict the initial migration celerities of infinitesimal bed perturbations. For longer bed perturbations (L=3,000 m) both approaches are accurate for Froude numbers up to and including F=0.3. For larger Froude numbers, the spatial-mode analysis excellently represents the initial migration celerities and provides an upper limit for the subsequent migration celerities of bed perturbations. The temporal-mode analysis gives somewhat smaller migration celerities, matching better to the migration celerities that occur later in the simulation. Therefore, the temporal mode proves more suitable for longer-term prediction of bed disturbance celerities.

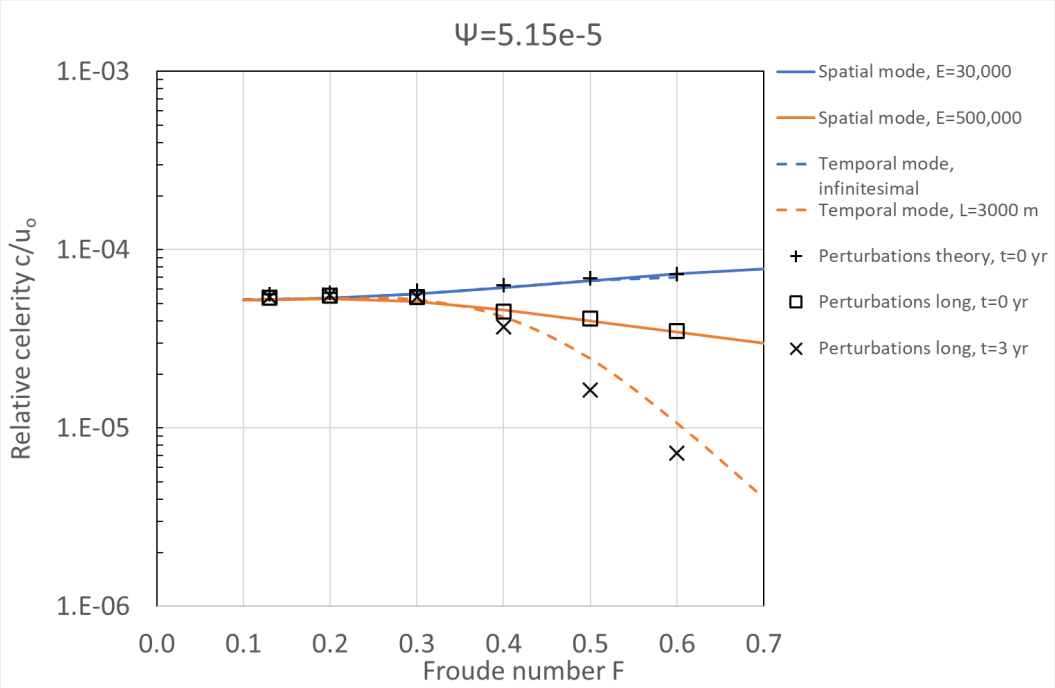


Figure 13. Migration celerities according to the linear stability analysis based on spatial and temporal modes for short and long bed waves, compared to simulated results.

In the domain where analytical models represent the exact solution, they can be used to verify the discretization approach and solution method in numerical models. For infinitesimal and matching perturbations of flow and the riverbed (Section 2.3.4), the analytical approach provides the exact solution of initial migration celerity and damping of water and bed waves. This provides valuable validation material for any one-dimensional modelling system, to test whether the processes are correctly implemented, the numerical scheme is appropriate and the numerical parameters and time and space step are properly selected.

For small and moderate Froude numbers ($F \leq$0.3), the linear stability analysis provides a good first estimate for small perturbations, but underestimates the migration celerities when bed waves become larger, and non-linearity and diffusion increase (see Figure 10). Figure 14 shows an example of the ratio of the migration celerity of a bed wave

from numerical simulations and migration celerity from the linear stability analysis, based on spatial modes. A value of 1 on the vertical axis means a perfect match. The horizontal axis shows the relative amplitude of the bed wave, which is defined as the ratio between the amplitude of the bed wave and the undisturbed water depth. For a bed wave of 1 m high and a water depth of 4 m, the multiplication factor is almost 4 for the initial migration celerity, and halves after 3 years. The multiplication factor shows an almost linear relation with relative wave amplitude for the initial value of the migration celerity, and this relation flattens for longer simulation times. G. Seminara (pers. comm.) suggested that, due to the quasi-linear dependence of the multiplication factor on the relative amplitude, a weakly nonlinear analysis might be successful in extending theoretical predictions beyond the linear approximation. Indeed, this could be worth considering.

The relations derived from Figure 14 could be used as a first pass for the correction factor of the migration celerity of the linear stability analysis, although it is based on simulations for one Froude number only, and general applicability has not yet been proven. The impact of a flood wave as upstream boundary (Figure 1) is shown by the open squares in Figure 14. The impact is negligible at t=0 because the discharge is equal to the undisturbed discharge and therefore water depth and flow velocity assume the undisturbed values. After 3 years, the overall migration celerity increased compared to the initial migration celerity, due to higher flow velocities and sediment transport rates during flood periods. For realistic flood wave conditions, the appropriate choice of the parameters E, F and Ψ therefore becomes less straightforward, even more so when flood waves dampen in the downstream direction.

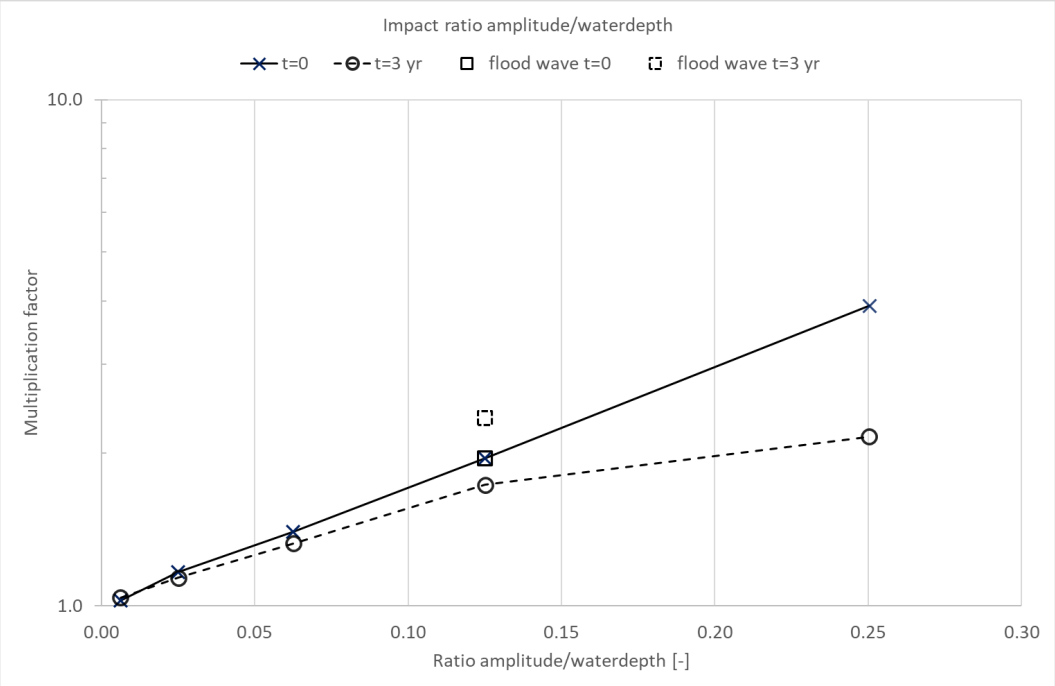


Figure 14. Ratio between simulated perturbation migration celerities and corresponding migration celerities from linear stability analysis as a function of bed wave amplitude to water depth ratio for F=0.2.

In the Dutch main rivers, morphological changes are ongoing due to historical works and changes of many kinds. New plans are being developed and climate is changing. To

assess the impact on riverbed morphology, long-term predictions are required. The linear stability analysis allows for a rapid assessment of how fast bed waves, induced by changed boundary conditions or measures, travel through the river, and indicate when they may cause problems and require management efforts at downstream locations. The Meuse River is used as an example for assessment of the applicability. In the downstream part of the river, where the bed slope is small and multiple weirs have been implemented, Froude numbers are moderate (on average 0.2 or lower), even during floods. In the upstream part of the Dutch Meuse River, referred to as the Common Meuse, slopes are 5 times higher, the river is free flowing, and the Froude numbers can take a value of up to 0.5, or locally even higher. This means that the analytically derived bed wave migration celerity will be an overestimation in the Common Meuse, because diffusion is high and wave lengths of bed waves are important (reflected in values of E). These wave lengths will change in time. In the downstream part of the Meuse River, bed waves have a translating character and the linear stability analysis provides a good estimate of the migration celerity of low-amplitude bed waves with various wave lengths.

For the Meuse River insufficient data were available to check the results of the linear stability analyses. Two other cases were selected for which field data on celerities of bed waves are available: the Fraser River in Canada and the Waal River in the Netherlands. The complete analyses for both rivers are presented in the supplementary material. Along the Fraser River, gold mining between 1858 and 1909 added large amounts of sediment to the river's natural sediment load. Ferguson et al. (2015) and Nelson and Church (2012) reconstructed the impact of the additional sediment supplies on the morphodynamics. Nelson and Church (2012) estimated that the annual travel distance of placer mining sediment was most likely 3.1 km in the Fraser River between Marguerite and Hope. The linear stability analyses are based on an average bed slope of 0.001, a Froude number at mean annual flood in the range 0.45-0.56 and an annual bed material load of 700,000 m^3. According to both spatial mode and temporal mode analyses, the propagation celerity is in the range of 2.25-3.3 km/yr, which matches the most likely celerity according to Nelson and Church (2012).

The Waal River in the Netherlands is the main branch of the Rhine delta. The geometry of the river bed of the Waal River has been monitored every two weeks by multibeam surveys in the period from 2005 to 2020. These surveys provide detailed information on the propagation of bed waves. Gensen and Van Denderen (2022) performed a wavelet analysis on the 2 weekly measurements to filter out bed waves with lengths between 300 to 4,000 m. On the relatively straight Middle Waal section, the celerity of these bed waves appeared to be 1.1 to 1.4 km/yr. The linear stability analyses are based on data from Van Denderen and Van Hoek (2022) and Paarlberg and Schippers (2020) (average bed slope of 0.0001, Froude number equal to 0.15) and Frings et al. (2019) (annual bed material load of 333,333 m^3). Based on the flow conditions at the average river discharge for the period 2005-2021, the spatial mode and temporal mode analysis provide a propagation celerity of 1,222 m/yr, which is within the range of the measured values reported by Gensen and Van Denderen (2022).

Figure 11 shows that for the shorter bed waves of 107 m (F=0.1) to 446 m (F=0.6) (Section 2.3.4), damping in the numerical simulations exceeds the damping of the linear stability analysis when $F \leq 0.4$. For longer bed waves, linear stability analysis and numerical results agree much better. In the supplementary material it is shown that the damping length from the spatial-mode analysis and from the temporal-mode analysis match well in this range of the Froude number, and the choice of mode does not explain the deviations as found. The explanation could be related to numerical diffusion in ELV for shorter bed waves, which could be a subject of future study.

5 Conclusions

A spatial-mode linear stability analysis was performed of the one-dimensional Saint-Venant-Exner equations, with a focus on subcritical flow with Froude numbers F up to 0.6 and river bed waves with wave lengths larger than the water depth. The linear stability analysis has yielded explicit relations to estimate migration celerities and damping lengths of flow and bed perturbations. The results were compared to numerical model simulations with ELV, which in turn were verified by several additional model runs with SOBEK-RE. The comparison shows that migration celerities from the linear stability analysis and numerical results agree well for infinitesimal perturbations at t=0. Regarding the initial response of these infinitesimal perturbations of the flow and morphology, the linear stability analysis can be used to validate numerical modelling codes.

For Froude numbers exceeding 0.3, bed waves show an increasingly diffusive character, where wave length increases and migration celerities decrease in time. For these conditions, the linear stability analysis based on spatial modes provides an upper limit of the migration celerity of bed perturbations. A temporal-mode linear stability analysis proves more suitable for longer-term prediction of the migration celerity. When perturbations are higher or longer, attaining dimensions that are significant compared to water depth or the length of the backwater curve, non-linear processes prevail and the diffusive character gains strength. For Froude numbers up to 0.3, the theoretical migration celerities are a good estimate for perturbations even for longer periods of development, as long as the amplitudes of the bed waves are smaller than about 5% of the depth. When perturbations have larger amplitudes, the linear stability analysis underestimates the initial migration celerity by 50% or more, which is why a correction factor is required. This correction factor is shown to be exponentially dependent on the relative amplitude (the amplitude to water depth ratio). Application of a correction would extend the applicability range of the linear stability analysis as a rapid assessment tool, but this needs a broader validation.

For Froude numbers of 0.4 and higher, the diffusive character causes an overestimation of the bed wave migration celerities by the linear stability analysis in the longer term, especially in case of the spatial-mode analysis. At the same time, non-linearity causes an underestimation by the linear stability analysis. The net impact of diffusion depends on the balance of these two effects, and is likely dependent on the value of the Froude number. As an example, the linear stability analysis may be used as a rapid assessment tool for bed waves up to 0.5 m high in the lower part of the River Meuse, referred to as the Sand Meuse. In the upstream steeper part of the river, the Common Meuse, the Froude numbers are higher, diffusion is larger and the linear stability analysis based on spatial modes loses predictive power, especially when longer periods of development are considered.

The linear stability analyses were applied to the Fraser River in Canada and Waal River in the Netherlands. This shows that even when Froude numbers are as high as 0.56 the propagation celerities of bed waves can be assessed realistically when average flow conditions and annual sediment loads are known.

Acknowledgments

This work is a part of the research program Rivers2Morrow (2018-2023), which focuses on long-term development of the Dutch rivers. Rivers2Morrow is financed by the Directorate-General for Water and Soil and Directorate-General Rijkswaterstaat, both being a part of the Dutch Ministry of Infrastructure and Water Management. HKV and Deltares provide additional support. The authors thank the reviewers and editors for their valuable comments. Special thanks to Prof. G. Seminara (University of Genoa) for the support on the analysis and valuable ideas on simplifying the solution, leading to the result of Eq. 22 and Eq. 23. We thank Dr. M. Borsboom (Deltares) for his valuable input on nu-

merical aspects of one-dimensional models. Also, discussions with Dr. B. Vermeulen (Wageningen University & Research) on the translation and diffusion of bed waves were important for the analyses performed.

Data availability statement: Numerical simulations have been carried out with the numerical modelling package ELV. ELV is available in the open access repository of the Open Earth Tools managed by Deltares:
https://svn.oss.deltares.nl/repos/openearthtools/trunk/matlab/applications/ELV. For the simulations we used the version at Revision 16973 from Thursday 17 December, 2020 11:20:54. The input and (reworked) output of the simulations with ELV, presented in the Figures 8, 10, 11 and 13, are available through Barneveld (2022).

References

Ancey, C., & Heyman, J. (2014). A microstructural approach to bed load transport: mean behaviour and fluctuations of particle transport rates. *Journal of Fluid Mechanics*, *744*, 129–168.

Arkesteijn, L., Blom, A., Czapiga, M. J., Chavarrías, V., & Labeur, R. J. (2019). The quasi-equilibrium longitudinal profile in backwater reaches of the engineered alluvial river: A space-marching method. *Journal of Geophysical Research: Earth Surface*, *124*(11), 2542–2560.

Arkesteijn, L., Blom, A., & Labeur, R. J. (2021). A rapid method for modelling transient river response under stochastic controls with applications to sea level rise and sediment nourishment. *Journal of Geophysical Research: Earth Surface*, e2021JF006177.

Balmforth, N., & Provenzale, A. (2001). Patterns of dirt. In *Geomorphological Fluid Mechanics* (pp. 369–393). Springer.

Barneveld, H. (2022). Supplementary information propagation of bed waves in rivers: ELV simulations and additional analyses, http://www.hydroshare.org/resource/7842147db84d4265b95fe2872132aa4a.

Blom, A., Arkesteijn, L., Chavarrías, V., & Viparelli, E. (2017). The equilibrium alluvial river under variable flow and its channel-forming discharge. *Journal of Geophysical Research: Earth Surface*, *122*(10), 1924–1948.

Bohorquez, P., & Ancey, C. (2015). Stochastic-deterministic modeling of bed load transport in shallow water flow over erodible slope: Linear stability analysis and numerical simulation. *Advances in Water Resources*, *83*, 36–54.

Bohorquez, P., & Ancey, C. (2016). Particle diffusion in non-equilibrium bedload transport simulations. *Applied Mathematical Modelling*, *40*(17-18), 7474–7492.

Bohorquez, P., Cañada-Pereira, P., Jimenez-Ruiz, P., & del Moral-Erencia, J. (2019). The fascination of a shallow-water theory for the formation of megaflood-scale dunes and antidunes. *Earth-science Reviews*, *193*, 91–108.

Bélanger, J. B. (1828). *Essai sur la solution numerique de quelques problemes relatifs au mouvement permanent des eaux courantes.* chez Carilian-Goeury, libraire, des corps royaux des ponts et chaussees et des mines.

Carraro, F., Vanzo, D., Caleffi, V., Valiani, A., & Siviglia, A. (2018). Mathematical study of linear morphodynamic acceleration and derivation of the MASSPEED approach. *Advances in Water Resources*, *117*, 40–52.

Charru, F. (2011). *Hydrodynamic instabilities* (Vol. 37). Cambridge University Press.

Chavarrías, V., Arkesteijn, L., & Blom, A. (2019). A well-posed alternative to the hirano active layer model for rivers with mixed-size sediment. *Journal of Geophysical Research: Earth Surface*, *124*(11), 2491–2520.

Chavarrías, V., Stecca, G., Siviglia, A., & Blom, A. (2019). A regularization strategy for modeling mixed-sediment river morphodynamics. *Advances in Water Resources*, *127*, 291–309.

Church, M., & Ferguson, R. (2015). Morphodynamics: Rivers beyond steady state. *Water Resources Research*, *51*(4), 1883–1897.

Colombini, M. (2022). Stability, resonance and role of turbulent stresses in 1d alluvial flows. *Environmental Fluid Mechanics*, 1–23.

Cui, Y., Parker, G., Lisle, T. E., Pizzuto, J. E., & Dodd, A. M. (2005). More on the evolution of bed material waves in alluvial rivers. *Earth Surface Processes and Landforms: The Journal of the British Geomorphological Research Group*, *30*(1), 107–114.

Dade, W. B., & Friend, P. F. (1998). Grain-size, sediment-transport regime, and channel slope in alluvial rivers. *The Journal of Geology*, *106*(6), 661–676.

De Vries, M. (1965). Considerations about non-steady bedload transport in open channels. In (pp. 3–8).

De Vries, M. (1966). Application of luminophores in sandtransport-studies.

De Vries, M. (1973). River bed variations-aggradation and degradation. In *Proc. int. seminars on hydr. of alluvial streams, iahr, delft, the netherlands* (pp. 1–10).

De Vries, M. (1975). A morphological time-scale for rivers. In *Deltares publication nr. 147, paper presented at the XVIth IAHR congress, São Paulo.*

Drazin, P. G., & Reid, W. H. (2004). *Hydrodynamic stability.* Cambridge University Press.

Engelund, F., & Hansen, E. (1967). A monograph on sediment transport in alluvial streams. *Teknisk Forlag, Kopenhagen.*.

Ferguson, R., Church, M., Rennie, C., & Venditti, J. (2015). Reconstructing a sediment pulse: Modeling the effect of placer mining on Fraser River, Canada. *Journal of Geophysical Research: Earth Surface*, *120*(7), 1436–1454.

Frings, R., Hillebrand, G., Gehres, N., Banhold, K., Schriever, S., & Hoffmann, T. (2019). From source to mouth: Basin-scale morphodynamics of the Rhine River. *Earth-science reviews*, *196*, 102830.

Furbish, D. J., Haff, P. K., Roseberry, J. C., & Schmeeckle, M. W. (2012a). A probabilistic description of the bed load sediment flux: 1. theory. *Journal of Geophysical Research: Earth Surface*, *117*(F3).

Furbish, D. J., Haff, P. K., Roseberry, J. C., & Schmeeckle, M. W. (2012b). A probabilistic description of the bed load sediment flux: 1. theory. *Journal of Geophysical Research: Earth Surface*, *117*(F3).

Gensen, M., & Van Denderen, R. (2022). Propagation celerity bed disturbances using bed level soundings rhine and waal, in dutch: Loopsnelheid bodemverstoringen - op basis van vaargeulpeilingen bovenrijn/waal. *Report HKV, PR4597.10, March 2022*.

Grijsen, J., & Vreugdenhil, G. (1976). Numerical representation of flood waves in rivers. *Proc. Int. Symp. Unsteady flow in open channels, Newcastle-upon-Tyne, BHRA Fluid Eng., Cranfield,*.

James, L. A. (2006). Bed waves at the basin scale: implications for river management and restoration. *Earth Surface Processes and Landforms: The Journal of the British Geomorphological Research Group*, *31*(13), 1692–1706.

Ji, Z., De Vriend, H., & Hu, C. (2003). Application of SOBEK model in the Yellow River estuary. In *International conference on Estuaries and Coasts, Hangzhou, China. Retrieved from http://www. irtces. org/pdf-hekou/114. pdf.*

Kennedy, J. F. (1963). The mechanics of dunes and antidunes in erodible-bed channels. *Journal of Fluid mechanics*, *16*(4), 521–544.

Kennedy, J. F. (1969). The formation of sediment ripples, dunes, and antidunes. *Annual review of fluid mechanics*, *1*, 147–168.

Lajeunesse, E., Devauchelle, O., & James, F. (2018). Advection and dispersion of bed load tracers. *Earth Surface Dynamics*, *6*(2), 389–399.

Lajeunesse, E., Malverti, L., & Charru, F. (2010). Bed load transport in turbulent flow at the grain scale: Experiments and modeling. *Journal of Geophysical Research: Earth Surface*, *115*(F4).

Lanzoni, S., Siviglia, A., Frascati, A., & Seminara, G. (2006). Long waves in erodible channels and morphodynamic influence. *Water Resources Research*, *42*(6).

Lesser, G. R., Roelvink, J. v., Van Kester, J., & Stelling, G. (2004). Development and validation of a three-dimensional morphological model. *Coastal Engineering*, *51*(8-9), 883–915.

Lisle, T. E. (2007). 17 the evolution of sediment waves influenced by varying transport capacity in heterogeneous rivers. *Developments in Earth Surface Processes*, *11*, 443–469.

Lisle, T. E., Cui, Y., Parker, G., Pizzuto, J. E., & Dodd, A. M. (2001). The dominance of dispersion in the evolution of bed material waves in gravel-bed rivers. *Earth Surface Processes and Landforms*, *26*(13), 1409–1420.

Lyn, D. A., & Altinakar, M. (2002). St. Venant–Exner equations for near-critical and transcritical flows. *Journal of Hydraulic Engineering*, *128*(6), 579–587.

Martínez-Aranda, S., Murillo, J., & García-Navarro, P. (2019). A comparative analysis of capacity and non-capacity formulations for the simulation of unsteady flows over finite-depth erodible beds. *Advances in Water Resources*, *130*, 91–112.

Meyer-Peter, E., & Müller, R. (1948). Formulas for bed-load transport. In *IAHR 2nd meeting, Stockholm, Appendix 2.*

Morris, P. H., & Williams, D. J. (1996). Relative celerities of mobile bed flows with finite solids concentrations. *Journal of Hydraulic Engineering*, *122*(6), 311–315.

Nakagawa, H., & Tsujimoto, T. (1980). Sand bed instability due to bed load motion. *Journal of the Hydraulics Division*, *106*(12), 2029–2051.

Nakagawa, H., & Tsujimoto, T. (1984). Spectral analysis of sand bed instability. *Journal of Hydraulic Engineering*, *110*(4), 467–483.

Nelson, A. D., & Church, M. (2012). Placer mining along the fraser river, british columbia: the geomorphic impact. *Bulletin*, *124*(7-8), 1212–1228.

Paarlberg, A., & Schippers, M. (2020). Inverse modelling equilibrium effect of measures on main river bed: deriving dimensions of measures, in dutch: Inverse modellering evenwichtseffect maatregelen op zomerbedbodem: afleiden dimensies van maatregelen. *Memo, January 2020*.

Ponce, V., & Simons, D. (1977). Shallow wave propagation in open channel flow. *Journal of the Hydraulics Division ASCE, Vol 103, HY12, Proc. Paper 13392, pp1461-1476*.

Ribberink, J., & Van der Sande, J. (1985). Aggradation in rivers due to overloading-analytical approaches. *Journal of Hydraulic Research*, *23*(3), 273–283.

Roseberry, J. C., Schmeeckle, M. W., & Furbish, D. J. (2012). A probabilistic description of the bed load sediment flux: 2. particle activity and motions. *Journal of Geophysical Research: Earth Surface*, *117*(F3).

Sieben, J. (1996). One-dimensional models for mountain-river morphology. *Communications on hydraulic and geotechnical engineering, No. 1996-02*.

Sieben, J. (1999). A theoretical analysis of discontinuous flow with mobile bed. *Journal of Hydraulic Research*, *37*(2), 199–212.

Sutherland, D. G., Ball, M. H., Hilton, S. J., & Lisle, T. E. (2002). Evolution of a landslide-induced sediment wave in the Navarro River, California. *GSA Bulletin*, *114*(8), 1036–1048.

USDA, N. (2007). *National engineering handbook hydrology, chapter 16, hydrographs.* United States Department of Agriculture, Natural Resources Conservation Service.

Van Denderen, R., & Van Hoek, M. (2022). Wavelet application, help documentation, in dutch: Waveletapplicatie, helpdocumentatie. *Report HKV, PR4591.10, March 2022*.

Van Vuren, S., Vriend, H. J. D., Ouwerkerk, S., & Kok, M. (2005). Stochastic modelling of the impact of flood protection measures along the river Waal in the

netherlands. *Natural Hazards*, *36*(1), 81–102.

Vreugdenhil, C. (1982). Numerical effects in models for river morphology. *Engineering applications of computational hydraulics*, *1*, 91–110.

Yossef, M. F., Jagers, H., Van Vuren, S., & Sieben, J. (2008). Innovative techniques in modelling large-scale river morphology. In *River Flow 2008, Proc. of the Intern. Conf. on Fluvial Hydraulics, Çeşme, Izmir, Turkey* (pp. 1065–1074).

WATER RESOURCES RESEARCH

Supporting Information for

Can linear stability analyses predict the development of river bed waves with lengths much larger than the water depth?

H.J. Barneveld[1,4], E. Mosselman[2,3], V. Chavarrías[2], A.J.F. Hoitink[1]

[1]Wageningen University and Research, Hydrology and Quantitative Water Management Group, Department of Environmental Sciences, Droevendaalsesteeg 3, 6708 PB Wageningen, the Netherlands

[2]Deltares, P.O. Box 177, 2600 MH Delft, the Netherlands

[3]Delft University of Technology, Faculty of Civil Engineering and Geosciences, P.O. Box 5, 2600 AA Delft, the Netherlands

[4]HKV, Botter 11-29, 8232 JN Lelystad, the Netherlands

Contents of this file

Text S1 to S4
Figures S1 to S7
Tables S1 to S2

Introduction

This document contains information on the numerical cases performed with the code ELV (S1), analysis on the impact of another choice of parameters (S2), a comparison between the damping length based on the temporal-mode analysis and spatial-mode analysis (S3) and two field cases to which the results are applied (S4).

Corresponding author: Hermjan Barneveld, (hermjan.barneveld@wur.nl)

Text S1 – Model cases

Table S1 shows the case names for the different simulations presented in Figures 8, 10, 11 and 13 of the manuscript.

Table S1. Cases performed in the study

	Cases, see legend in the Figures in the manuscript				
	Ψ = 5.15 E-4				Ψ = 2 E-4
	Perturbations theory, t=0yr	Perturbations long, t=0yr	Perturbations long, t=3yr	Perturbations large&long, Qwave, t=3yr	Perturbations theory, t=0yr
Froude number *F*	*Figures 8, 11, 13*	*Figures 8, 11, 13*	*Figures 8, 11, 13*	*Figures 8, 10*	*Figure 8*
0.13	006dXSS2bdyn	006dXSdyn	006dXSdyn	003d25Gdyn	006dXSS3bdyn
0.2	019dXSS2bdyn	019ddyn	019ddyn	013dxGdyn	019dXSS3bdyn
0.3	015dxSmXSS2bdyn	015dxSmdyn	015dxSmdyn	015dxGdyn	015dxSmXSS3dyn
0.4	017dXSS2cdyn	017ddyn	017ddyn	016dGdyn	017dXSS3dyn
0.5	016d5SmXSS2cdyn	016d5Smdyn	016d5Smdyn	016d5Gdyn	016d5SmXSS3dyn
0.6	011dx10aD35XSS2ddyn	018dadyn	018dadyn	011dx10aD35Gdyn	011dx10aD35XSS3dyn

For the assessment of the impact of the choice of the Chézy value on the migration celerity (while keeping the parameters *F* and Ψ equal), the following additional simulations have been performed (*F*=0.2 and Ψ =5.15E-5).

- 013DXG2 with *C*=40 $m^{1/2}/s$, *D50*=0.009 m, i_b=0.000245 [-]
- 013DXG2a with *C*=45 $m^{1/2}/s$, *D50*=0.00633 m, i_b=0.0001936 [-].

Results of this analysis can be found in the Section S2 (Impact of the Chézy value).

The input and output of the model runs can be found in the Hydroshare Resource:

Barneveld, H. (2022). Supplementary information propagation of bed waves in rivers: ELV simulations and additional analyses, HydroShare, http://www.hydroshare.org/resource/7842147db84d4265b95fe2872132aa4a

It contains the following documents:

- The Resource contains following files per case:
- beddev.xlsx - bed level as a function of time and space
- beddev_dyn_'name'.xlsx - analysis of beddev.xlsx to assess celerities and generate graphs
- cpu.txt - output cpu time simulation
- input.mat - Matlab input file for ELV
- log.txt - log file simulation
- output.mat - matlab output file ELV

Text S2 – Impact of the Chézy value

Changing the Chézy value, while maintaining the same values for water depth, velocity, Froude number F and transport parameter Ψ, requires changes in the bed slope and D_{50}, and causes changes in the parameter E. The linear stability analysis demonstrates the impact of these changes on the relative migration celerity and damping of bed waves. For small Froude numbers (<0.3) the impact of changes in bed slope, D_{50} and E on the migration celerity is negligible, as can be seen in Figure S1 (for F≤0.3 lines overlap).

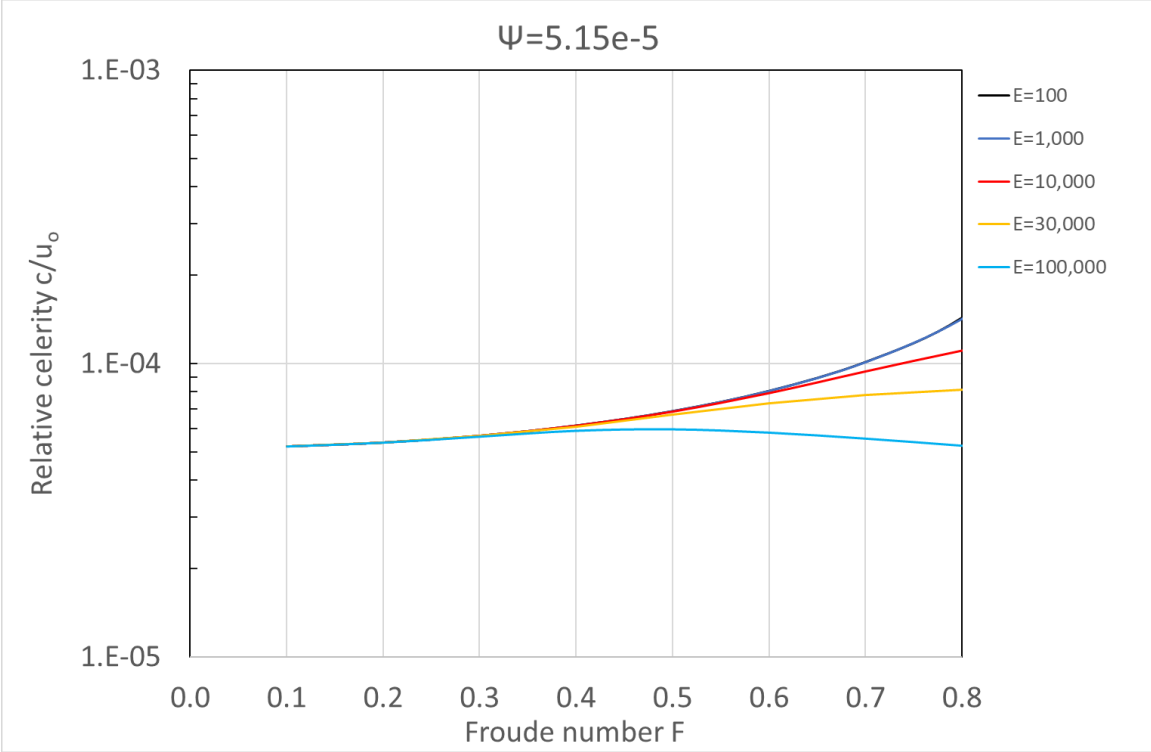


Figure S1. Relative celerity of bed waves in the linear stability analysis for Ψ = 5.15·10−5 (Figure 3 of manuscript).

We performed additional simulations in which we changed the Chézy value, as well as the values for i_b, and D_{50} so as to maintain the same values for F and Ψ. Table S2 gives the parameters as chosen, as well as the parameter values that result from these choices.

Table S2. Cases for sensitivity analysis for changed conditions for C, D_{50} and i_b.

parameter	Original simulation Case 013DXG2	Changed condition Case 013DXG2a
C (m1/2/s)	40	45
F (-)	0.2	0.2
Ψ (-)	5.15E-5	5.15E-5
i_b (slope)	0.000245	0.0001936
D_{50} (m)	0.009	0.00633

The results of both simulations, in terms of bed level change relative to the original bed slope ($i_{b,o}$), are presented in Figure S2. It can be seen that although the sediment loads appear to differ slightly, and the rates of diffusion in both simulations are somewhat different, the migration celerities (identified at the top of the wave) are almost identical. While keeping F and Ψ the same, other choices of parameters yield identical results for the migration celerity of the wave, as long as the results are insensitive to changes in parameter E. This shows that the results of the linear stability analysis are valid, also in case of other parameter choices such as for the Chézy value.

The small differences in damping and diffusion may be due to numerical diffusion in ELV, which could be subject to further research.

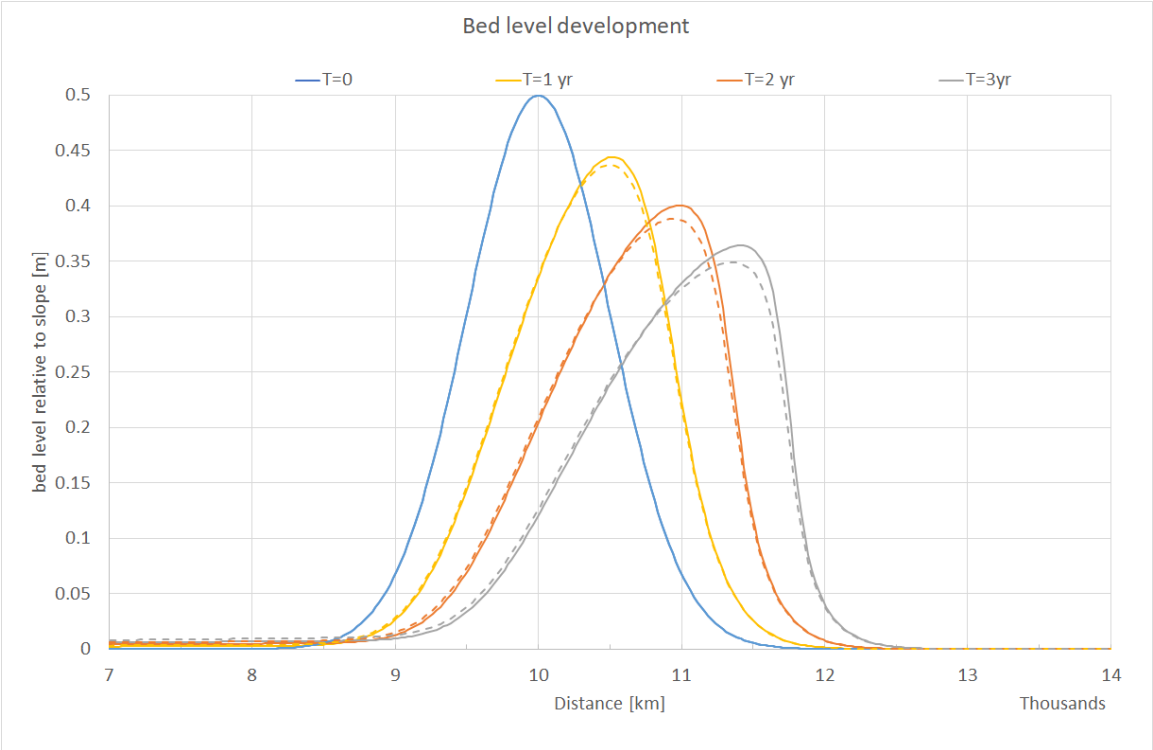


Figure S2. Comparison of dynamic of bed wave for alternative choices of C, D_{50} and i_b. Solid lines: base case 013DXG2; dashed lines: changed conditions case 013DXG2a.

Text S3 – Damping : Temporal-mode versus Spatial-mode

The damping or relaxation length are calculated in the spatial-mode analysis according to Eq. 16 in the main manuscript. For the temporal-mode analysis, the damping length can be calculated as follows. Suppose the peak of a wave travels with celerity c over a distance X. The corresponding travel time is $T_{Travel} = \frac{X}{c}$. The damping of the peak during this travel time is given by $\exp(\omega_i T_{travel}) = exp\left(\frac{\omega_i X}{c}\right)$, with damping factor ω_i and celerity c resulting from the temporal-mode analysis. This damping must also be equal to $exp\left(-\frac{X}{L_D}\right)$, where L_D denotes the damping length. Hence, $exp\left(\frac{\omega_i X}{c}\right) = exp\left(-\frac{X}{L_D}\right)$, which implies $L_D = -\frac{c}{\omega_i}$.

Plotting this for the damping length L_D in Figure 11 of the manuscript provides Figure S3.

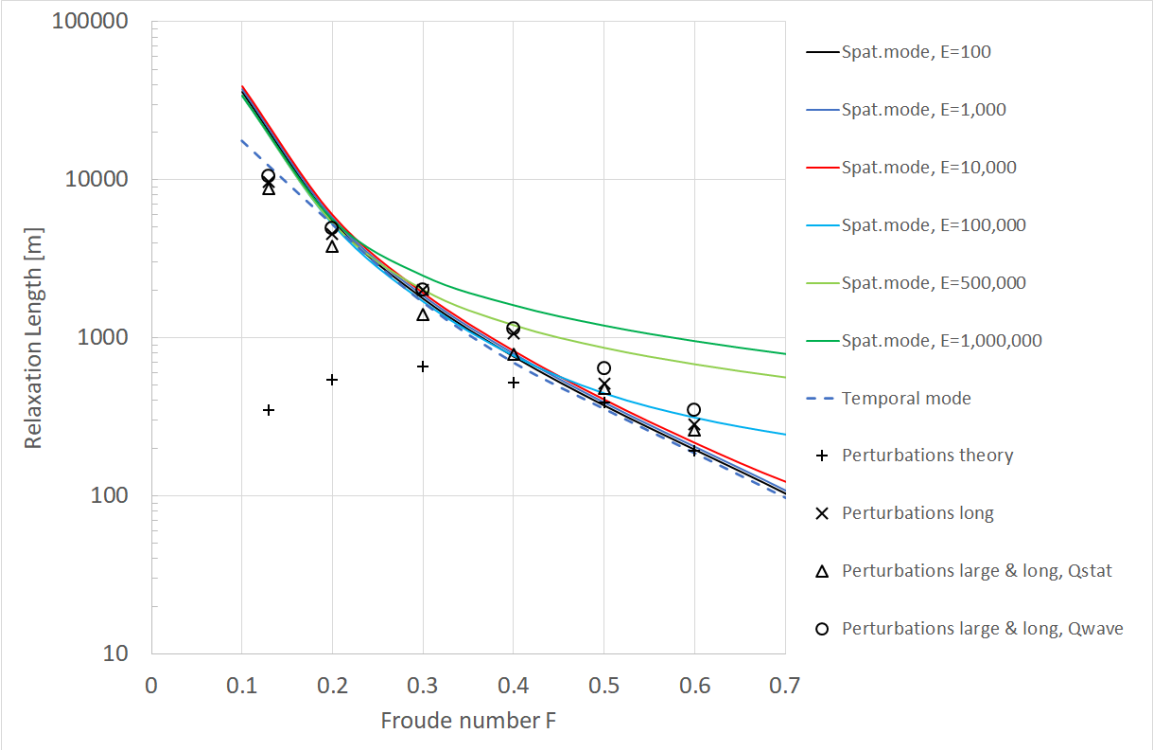


Figure S3. Comparison between damping of bed perturbations from linear stability analysis (solid lines for the spatial-mode, dotted line for the temporal-mode) and numerical simulations (markers) for $\Psi = 5.15 \cdot 10^{-5}$. 'Perturbations theory' represent infinitesimal perturbations with a wave length coupled to the value of E. For the other simulations, the wave length increased to 3,000 m, while for 'Perturbations large & long, Qwave' the bed wave amplitude increased and a flood wave was applied.

The figure shows that the results from the temporal-mode analysis are close to those from the spatial-mode analysis, for values of the parameter E up to 1,000.

However, for low values of the Froude number (F<0.2) the damping according to the temporal-mode analysis is somewhat larger (smaller value of L_D) than the damping from the spatial-mode analysis, and close to the numerical results for longer bed perturbations (x,Δ,o). For F>0.2 the value of the parameter E in the spatial-mode analysis becomes important and the damping-length of the temporal-mode analysis appears to give the lower limit for both spatial-mode analysis results and the numerical results for long bed perturbations.

The comparison to numerical results needs further research, including the impact of numerical diffusion in ELV.

Text S4 – Field cases: Fraser River (Canada) and Waal River (the Netherlands)

To illustrate the applicability of the linear stability analysis results, two cases with relevant field data for rivers in Canada and the Netherlands are addressed.

Gold mining along the Fraser River between 1858 and 1909 added large amounts of sediment to the river's natural sediment load. Ferguson et al. (2015) and Nelson & Church (2012) reconstructed the impact of the additional sediment supplies on the morphodynamics.

The Waal River in the Netherlands is the main branch of the Rhine delta. The geometry of the river bed of the Waal River has been monitored every two weeks in the period 2005 and 2021. This monitoring material provides detailed information on the migration of bed waves with various wave lengths. Results of these analyses are documented by Gensen & van Denderen (2022).

Fraser River, Canada

The sediment pulse of place mining on the Fraser River has been analyzed by Ferguson et al. (2015) and Nelson & Church (2012) using observations of the Fraser River channel and numerical modelling. Based on these studies, the following data for the reach between Marguerite and Hope were extracted:

- An average bed slope i_o of 0.001 (Ferguson et al., 2015);
- A steady dominant discharge of 7,000 m^3/s operating 15% of the time predicts the total flux of sediment, grain size distribution and net morphological changes for a 20-year period with annual peaks ranging from 6,070 to 12,900 m^3/s (Ferguson et al., 2015);
- An average channel width of 150 m (Ferguson et al., 2015);
- Froude numbers at mean annual flood of 0.45 at Hope and 0.56 at Marguerite (Nelson & Church, 2012);
- From 456 identified individual mines approximately 58,000,000 m^3 of sediment was excavated, and dumped into the Fraser River between the Cottonwood Canyon (upstream of Marguerite) and Hope (Nelson & Church, 2012);
- An annual travel distance of placer mining sediment (L_b) varying between 1 and 6.3 km/yr, with a most likely value of 3.1 km/yr (Nelson & Church, 2012);
- An annual delivery value of 700,000 m^3 of sediment, matching the most likely value of L_b (Nelson & Church, 2012).

These values were used in the linear stability analyses to assess the migration celerities, both for the spatial mode and the temporal mode approach. In those analyses, a Froude number of 0.5 was adopted as an average. As no information was readily available on flood wave periods (which determine parameter E in spatial mode analysis) and wave length L of the bed waves (parameter in temporal mode analysis) these parameters were varied (Figure S4). If the flood duration would be as long as 15% of time over a year (55 days), the parameter E would be approximately 19,000. Therefore, values of E larger than 100,000 are unlikely for the Fraser River. A bed wave with a wave

length L of 25 km or larger would slow down the bed wave to 1 km/yr, or less. Multiple bed waves (with shorter wavelengths, i.e. <10 km) may have moved through the system. Based on the latter assumptions, the migration celerities are in the range 2.25-3.3 km/yr (Figure S4).

The Froude numbers are larger than 0.3-0.4, and therefore, both transition and diffusion may be expected in this part for the Fraser River. Notwithstanding this expected behavior, we conclude that the results of both spatial mode and temporal mode analyses are close to the most likely bed wave migration celerity in this river (3.1 km/yr).

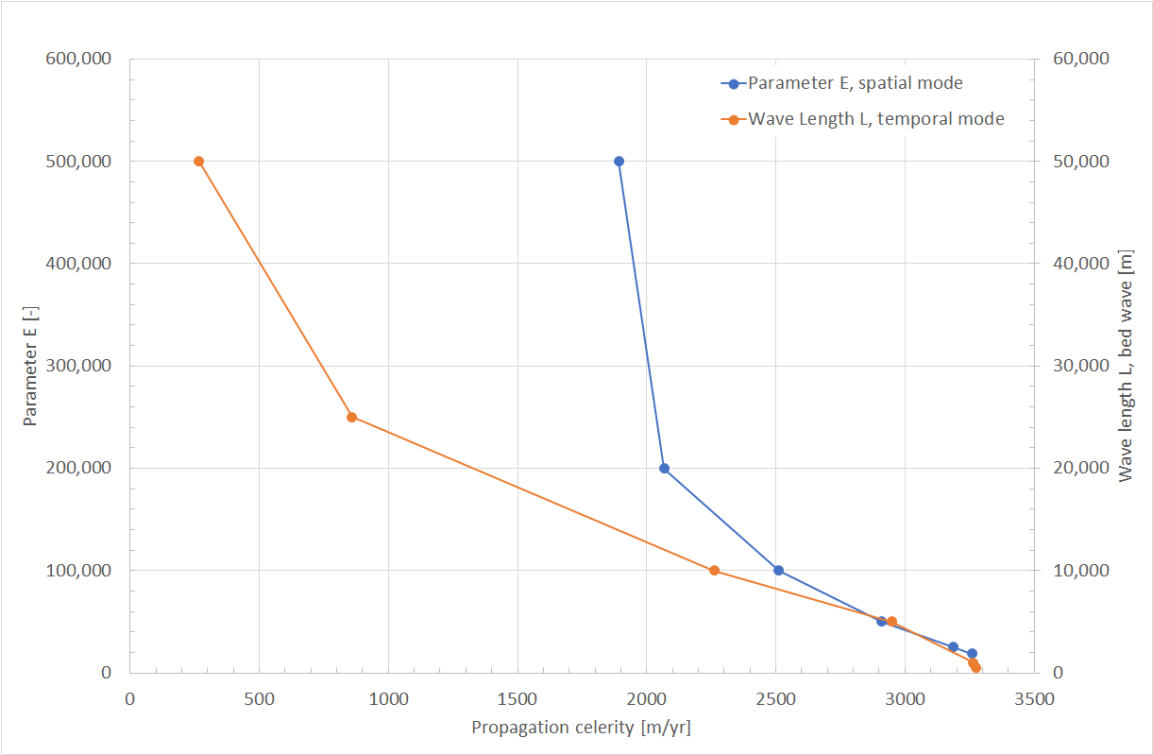


Figure S4. Sensitivity analysis on the impact of the parameter E (spatial mode analysis) and wave length bed wave L (temporal mode analysis) on the migration celerity of the bed wave. Fixed parameter settings are i_o=0.001, discharge Q=7,000 m^3/s, channel width W=150 m, annual sediment load S=700,000 m^3 and Froude number F=0.5.

Waal River, The Netherlands

The Rhine River enters the Netherlands near the village of Lobith. After approximately 10 km, it bifurcates in the Waal River and the Pannerden Canal. The Waal River flows to the west towards the Rhine-Meuse Delta, in which the large harbor of Rotterdam is situated. The Waal River and Rhine River are of high importance for navigation. The riverbed of these rivers is monitored frequently to assess the navigation depth and to plan dredging activities. In the period 2005-2021, the bed level of the navigation channel has been monitored every two weeks, which means that a large database is available to analyze morphodynamics of the river.

Van Denderen et al. (2022) use these detailed bed level measurements to study the morphological changes on multiple scales using a wavelet transform. A wavelet transform distinguishes and disentangles the bed-level changes on different spatial scales. In this way, the bed level change caused by a local intervention can be separated from larger scale changes. Gensen and Van Denderen (2022) applied this method to filter out bed waves with lengths between 300 m and 4 km. Such bed waves may be initiated by changes in river geometry, combined with flood events. These bed waves subsequently migrate downstream. An example of the result of the wavelet tool can be seen in Figure S5, clearly showing the downstream migration of longer bed waves.

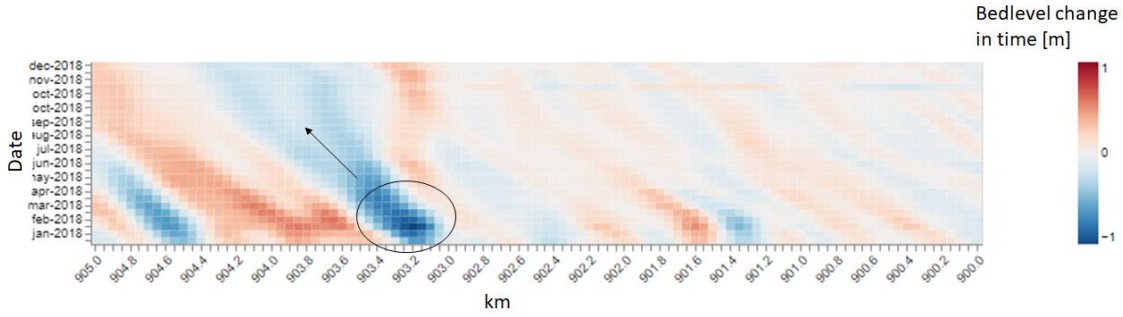


Figure S5. Bed level change for part of the Waal River in the year 2018. Clearly, the downstream migration of bed level peaks (red) and troughs (blue) can be distinguished. Water flows from right to left. Source: Van Denderen and Van Hoek (2022).

For comparison of the observed migration celerities, with results of the linear stability analyses, we selected a part of the Waal River which is called the Middle Waal in the reach km 887-915, see Figure S6. This reach is relatively straight and the migration celerities appear to be quite stable in time. For this section, Gensen & Van Denderen (2022) determined an annual travel distance of the bed waves varying between 1.1 and 1.4 km/yr .



Figure S6. Rhine and Waal River in the Netherlands. The Rhine enters the Netherlands near Lobith. Downstream from the bifurcation at the Pannerdensche Kop (km 867.5) the Waal River flows to the West. Downstream from the city of Nijmegen, the river is called the Middle-Waal.

Frings et al. (2019) provide an estimate of the annual sediment load for the Waal River of 200,000 m^3 excluding pores (±50%), or 333,333 m^3 (±50%) including pores. Other input parameters for the linear stability analyses are based on the discharge time-series at

Lobith (Figure S7) for the period 2005-2021. This time-series is transformed into representative discharges, specific discharges (m^2/s), water depths, flow velocities and Froude numbers based on:

1. The distribution of the river discharge at the bifurcation;
2. Water level slope;
3. Average cross-sectional shape containing width of the main section, relative height of the groynes and floodplains;
4. The discharge distribution in the cross-sectional profile (main section, groyne section, floodplain) extracted from numerical model results.

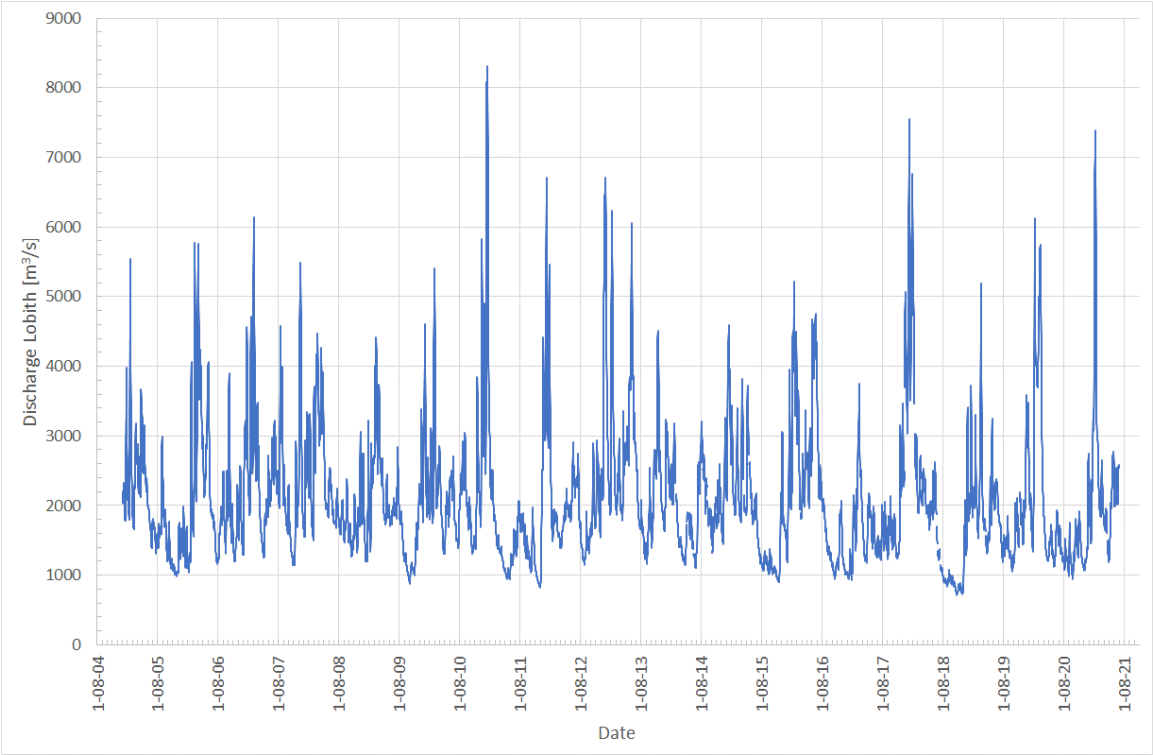


Figure S7. Discharge time-series at Lobith for the period January 2005 to July 2021.

This information, combined with river characteristics from Paarlberg & Schippers (2020), yields the following input parameters for the linear stability analyses:

- An average bed slope i_o of 1.10^{-4};
- The average discharge at Lobith in the observation period is approximately 2,000 m^3/s. For the analyses we adopted this discharge level as well as discharge levels of 1,600 m^3/s (overtopping of groynes) and 3,000 m^3/s;
- With information from Paarlberg & Schippers (2020), for the three discharge levels (1,600, 2,000 and 3,000 m^3/s), we determined the corresponding total discharges in the Waal (1,268, 1,461 and 2,049 m^3/s), the discharges in the

main river (between the groynes) (1,268, 1,432 respectively 1,900 m^3/s), and water depth (5, 5,5 and 6,5 m);
- An average channel width of 253 m;
- Froude number of 0.15;
- An annual sediment load of 333,333 m^3.

Based on this input, the wave celerities in both spatial mode and temporal mode analysis were calculated. We varied the characteristic discharge at Lobith (and the Waal River) and the wave length of the bed wave. Figure 2 in the manuscript shows that for Froude numbers of 0.15, the results are insensitive to the value of the parameter *E*.

The results with varying wave length *L* of the bed wave (a parameter only in temporal mode) showed insensitivity in the range *L*=300-4000 m. The discharge at Lobith does exert an influence. When the annual sediment load remains unchanged (333,333 m^3/yr), the travel distance L_b is 1,345 m/yr when the discharge at Lobith is 1,600 m^3/s. For discharges at Lobith equal to 2,000 m^3/s (mean discharge) and 3,000 m^3/s, L_b reduces to 1,222 and 1,035 m/yr, respectively. Differences in results of the spatial mode and temporal mode are negligible.

Choosing an average discharge (2,000 m^3/s) apparently provides a good approximation of the observed annual travel distance of 1.1 and 1.4 km/yr. Adopting low (1,600 m^3/s) or high (3,000 m^3/s) estimates of the discharge at Lobith yield bed wave celerities matching the observed values, but at the borders of the band width of the observations. It should be realized that the annual sediment load was identical for the three discharge values (333,333 m^3/yr). It can be concluded that adopting a correct value for the annual sediment load is more important than the selected value of the discharge, as the celerity appears to be linearly dependent on the sediment load.

REFERENCES

Ferguson, R. I., M. Church, C. D. Rennie, and J. G. Venditti (2015), Reconstructing a sediment pulse: Modeling the effect of placer mining on Fraser River, Canada, J. Geophys. Res. Earth Surf., 120, 1436–1454, doi:10.1002/2015JF003491.

Frings, R. M., G. Hillebrand, N. Gehres, K. Banhold, S. Schriever, and T. Hoffmann (2019), From source to mouth: Basin-scale morphodynamics of the Rhine River, Earth-science reviews 196: 102830.

Gensen M. and R.P. van Denderen (2012), Propagation celerity bed disturbances using bed level soundings Rhine and Waal, in Dutch: "Loopsnelheid bodemverstoringen - Op basis van vaargeulpeilingen Bovenrijn/Waal", Report HKV, PR4597.10, March 2022.

Nelson A.D. and M. Church (2012), Placer mining along the Fraser River, British Columbia: The geomorphic impact, Geological Society of America Bulletin; July/August 2012; v. 124; no. 7/8; p. 1212–1228; doi: 10.1130/B30575.1

Paarlberg A. and M. Schippers (2020), Inverse modelling equilibrium effect of measures on main river bed: deriving dimensions of measures, In Dutch: "Inverse modellering evenwichtseffect maatregelen op zomerbedbodem: afleiden dimensies van maatregelen", 22 January 2020.

Van Denderen R. P. and M. van Hoek (2022), Wavelet application, Help documentation, in Dutch: "Waveletapplicatie, Helpdocumentatie", Report HKV, PR4591.10, March 2022.

Van Denderen R. P., E. Kater, L. H. Jans, and R.M. Schielen (2022), Disentangling changes in the river bed profile: The morphological impact of river interventions in a managed river. Geomorphology, 408, 108244.